Electronic Supplementary Material (ESI) for Green Chemistry.

SUPPORTING INFORMATION

Palladium nanodendrites uniformly deposited on the surface of polymers as an efficient and recyclable catalyst for direct drug modification *via* *Z*-selective semihydrogenation of alkynes.

José García-Calvo,[a] Patricia Calvo-Gredilla,[a] Saúl Vallejos,[a] José Miguel García,[a] José Vicente Cuevas-Vicario,[a] Gabriel García-Herbosa,[a] Manuel Avella,[b] Tomás Torroba*[,b]

[a] Department of Chemistry, Faculty of Science, University of Burgos, 09001 Burgos, Spain

[b] Advanced Microscopy Unit, Scientific Park Foundation, I+D Building, Miguel Delibes Campus, University of Valladolid, 47011 Valladolid, Spain

Experimental part:

Materials and methods. Solvents and reagents were obtained from commercial sources and used as received. Column chromatography: SiO_2 (40-63 μm) TLC plates coated with SiO_2 60F254 were visualized by UV light. NMR spectra were recorded at 25°C using a Bruker AC300 spectrometer. The solvents for spectroscopic studies were of spectroscopic grade and used as received. UV/Vis spectra were measured with a Helios Gamma spectrophotometer. IR spectra were recorded with a Nicolet Impact 400D spectrophotometer. High resolution Mass spectra were obtained from a Bruker Reflex II matrix-assisted laser desorption/ionization time of flight (MALDI-TOF) using dithranol as matrix and with a 6545 Q-TOF (Agilent) with ESI ionization. ICP mass analysis was provided with a ICP-MS Agilent Serie 7500 equipment. The TGA analysis were performed with a TGA Q50 model (TA Instruments) under nitrogen atmosphere.

Scanning Electron Microscopy (SEM) measurements have been carried out at the Microscopy Unit of the Scientific Park University of Valladolid by means of an Environmental Scanning Electron Microscope (ESEM), model FEI-Quanta 200FEG provided with a Schottky-Field Emission filament. The SEM analyses were performed at Low Vacuum Mode using water vapor as auxiliary gas. This imaging mode allows working with non-conductive samples without any specific preparation or metallic coatings. The working pressure in the chamber for these analyses ranged between 0.9 Torr up to 2 Torr. The SEM images were acquired with the Large Field Detector (LFD) which is the suitable one for secondary electron detection at low vacuum mode and with a SSD Detector for Backscattered Electron signal (BSED). The accelerating voltage for these measurements ranged between 4 to 10kV. For TEM characterization a JEOL JEM-1011HRP working at 100kV was used and for High Resolution TEM (HR-TEM) the equipment was a JEM-2200F working at 200kV of accelerating voltage. For the particle size characterization the ImageJ software was used. The Feret's diameter was used as a measurement parameter since particle shapes were irregular. XPS analysis was performed with a XPS Spectrometer Kratos AXIS Supra at a pressure inferior to 10^{-9} Torr, the instrument was provided by the Advance Microscopy Laboratory from the University of Zaragoza.

1. SYNTHESIS AND CHARACTERIZATION

The palladium salt chosen was $PdCl_2 \cdot 2NaCl$, dissolved in water, C = 5 mM.

The composition of the polymers was chosen within a variety of combinations of different monomers, a crosslinker and a photoinitiatior.

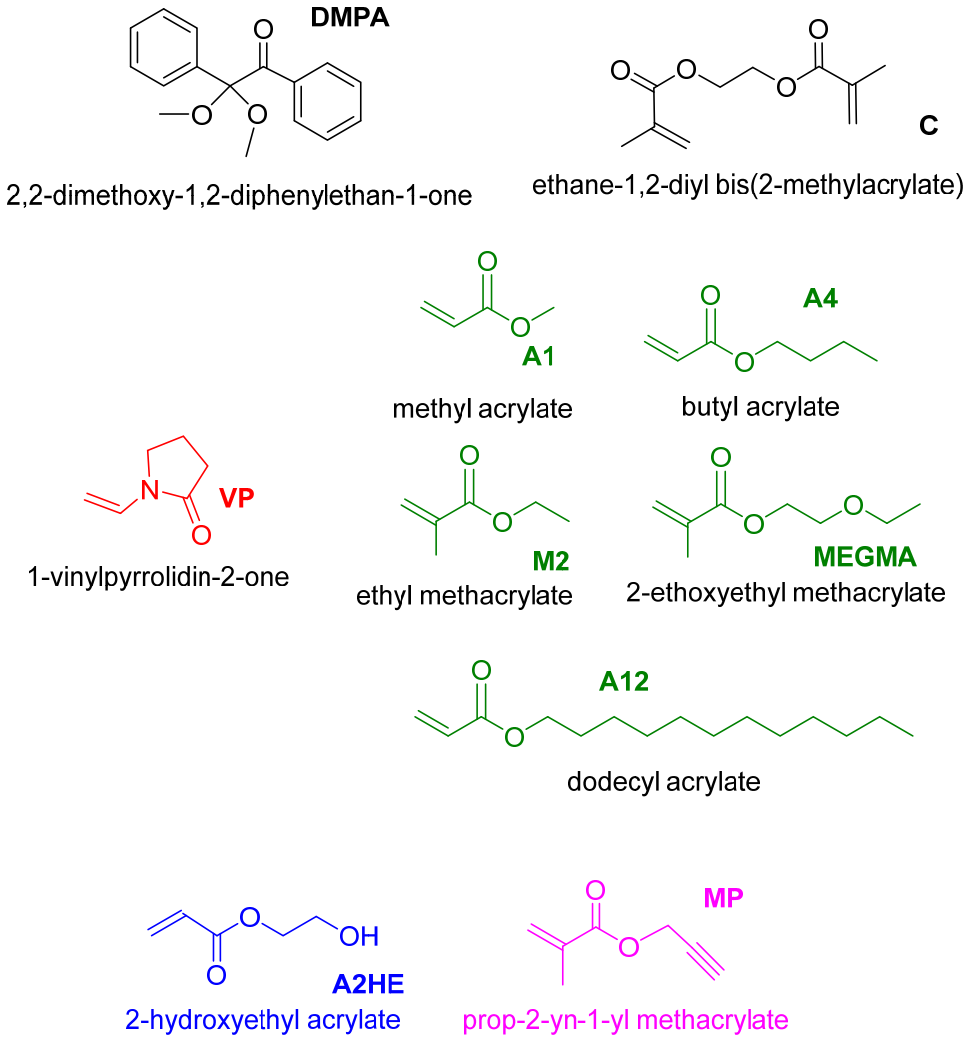

Figure S1. Components of the film monomers and photoinitiator (DMPA), "x", "y" and "z" represent the relations between components; x+y= 100%, z is the percentage respect x+y.

A series of polymers was developed to study the preparation of metal-modified polymers with new applications. $PdCl_2 \cdot 2NaCl$ is of particular interest due to the many possibilities of Pd as heterogenic catalyst being supported in a surface.

Several polymers were synthetized varying the co-monomers percentage, as it is indicated in the **Figure S1**. The compounds were characterized by IR, TGA, UV-Vis, SEM and EDX giving information about:

- TGA (Thermogravimetric analysis): stability of the polymers with temperature and how the presence of Pd affects their behaviour.
- IR (Infrared): determination of the characteristic bands in that region and possible variations in presence of Pd.
- SEM (scanning electron microscopy): the size and shape of the particles in the surface.
- EDX (Energy dispersive X-Ray spectroscopy): composition of the surface. The counterions in the palladium salts were chloride; as a consequence, the absence of this counterion means the absence of absorbed salt in the polymers.
- XPS (X-ray photoelectron spectroscopy): gives composition of the surface. The analysis is less deep than EDX; additionally it gives information about the oxidation state.
- UV-Vis absorption: by checking in literature[1], the presence of certain bands means the formation of nanoparticles of different sizes and shapes.

With all these techniques, the polymers were deeply studied and compared. **Figure S1** presents an overview of the components of every tested polymer.

Films (%)	VP	A12	A4	A1	M2	MEGMA	MP	A2HE	C
PBM2	50	x	x	x	50	x	x	x	0
PBMEGMA	50	x	x	x	x	50	x	x	0
PB0	60	x	40	x	x	x	x	x	0
PB20_80A12	20	80	x	x	x	x	x	x	10
PB20_80A4	20	x	80	x	x	x	x	x	10
PB20_80A1	20	x	x	80	x	x	x	x	10
PB0_100A4	x	x	100	x	x	x	x	x	10
PB0_100A1	x	x	x	100	x	x	x	x	10
PB80_20A1	80	x	x	20	x	x	x	x	10
PB80_20A4	80	x	20	x	x	x	x	x	10
A2HE5	x	x	x	x	x	x	x	100	10
JG25_SA2	x	x	x	x	x	x	5	95	10

Figure S2. Composition of the different studied polymers.

Visual appearance of the polymers:

These colourless films (1×1 cm) were put in a $PdCl_2$·2NaCl solution (5 mM, 3 mL) for 20 hours, and washed with water. Afterwards, changes in the polymer were observed for some of them:

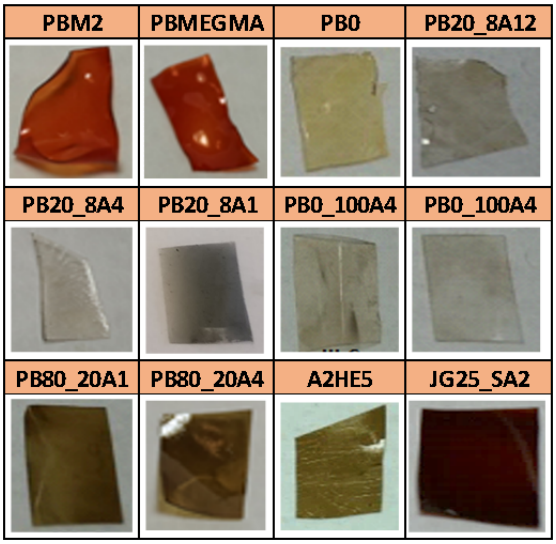

Figure S3. Pictures of the polymeric films after treated with a $PdCl_2$·2NaCl solution.

Three different behaviours were observed. The polymer remained unaffected, it took Pd(0) over their surface or it absorbed Pd(II), or a mixture of Pd(0)+Pd(II):

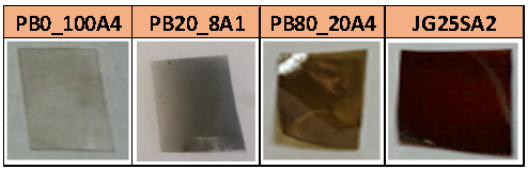

Figure S4. Visual appearance of the films after in presence of $PdCl_2$·2NaCl 5 mM for 20 hours. From left to right; no effect, Pd(0) and Pd(II) or Pd(0)+Pd(II).

- The polymers that contained only acrylate derivatives (PB0_100) or a high percentage of the acrylate with a long aliphatic chain (PB20_80A4 and PB20_80A12) did not experience any change after being in the presence of palladium solutions. The films remained colourless, first picture on Figure S4.
- PB20_80A1 presented a black layer over its surface; once analysed, it was concluded that they were Pd(0) nanoparticles. Second picture in Figure S4.
- PB0, PB80_20A4, PB80_20A1 and A2HE5 acquired orange-brown colours, showing mixtures of Pd(II) and Pd(0). Third picture in Figure S4.
- PBM2, PBMEGMA and JGSA2 acquired reddish colours. Afterwards, it was checked hat they also presented a mixture between Pd(II) and Pd(0). Fourth picture in Figure S4.

TGA analysis:

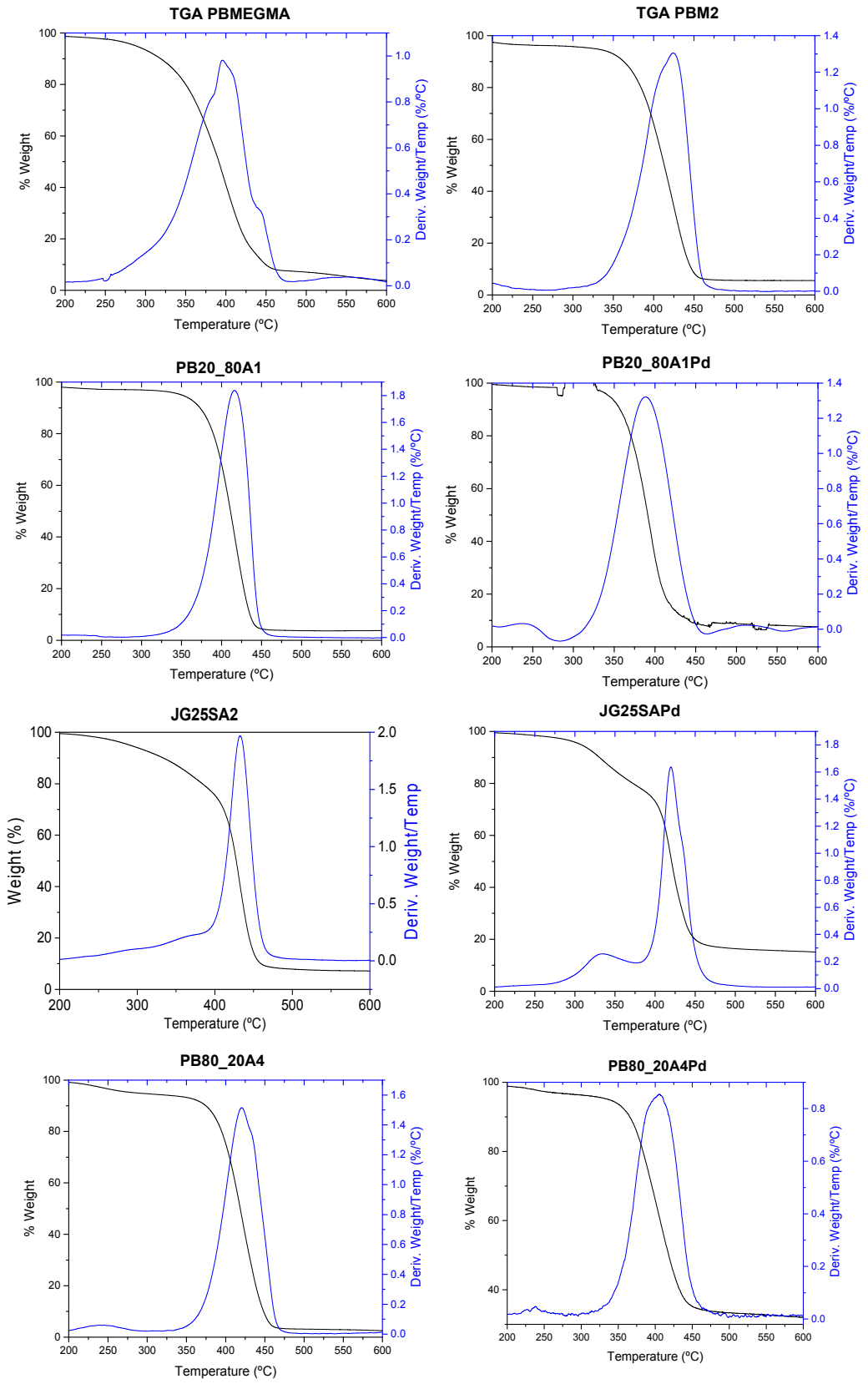

Figure S5. TGA analysis of the polymers

All the polymers had a total weight loss at around 430 ºC. In addition, there was no significant transitions due to the presence of palladium.

Infrared spectra

The IR spectra were measured for the different polymers synthesized (green). The IR was also measured after being in the presence of Pd^{2+} solution (blue), in order to observe possible changes in the spectra.

PB0

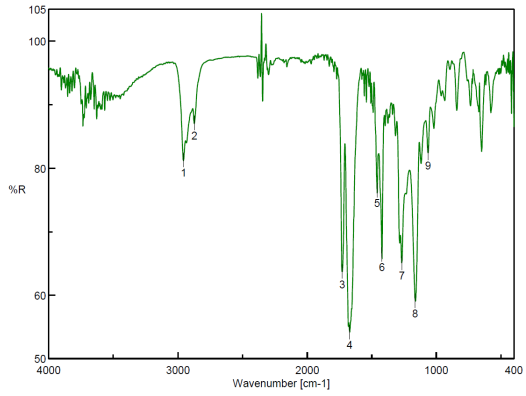

No.	Position	Intensity	No.	Position	Intensity
1	2955.38	81.2927	2	2871.49	87.1186
3	1728.87	63.6982	4	1670.05	54.1744
5	1458.89	76.503	6	1419.35	66.3805
7	1267.97	65.0587	8	1162.87	59.1085
9	1063.55	82.3814			

PB0_100A4

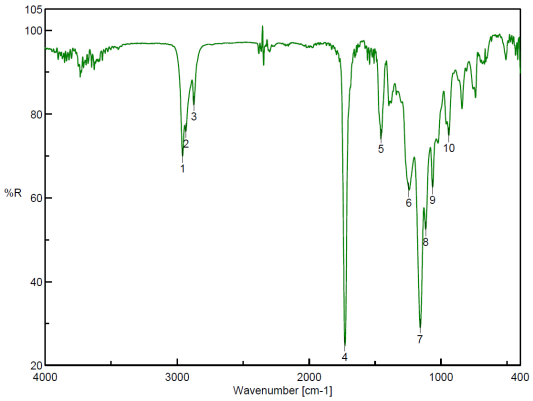

No.	Position	Intensity	No.	Position	Intensity
1	2957.3	70.0169	2	2932.23	75.9968
3	2871.49	82.4339	4	1728.87	25.0729
5	1454.06	74.7124	6	1242.9	61.8364
7	1159.01	29.3141	8	1115.62	52.5306
9	1063.55	62.5204	10	940.128	74.9085

PB05

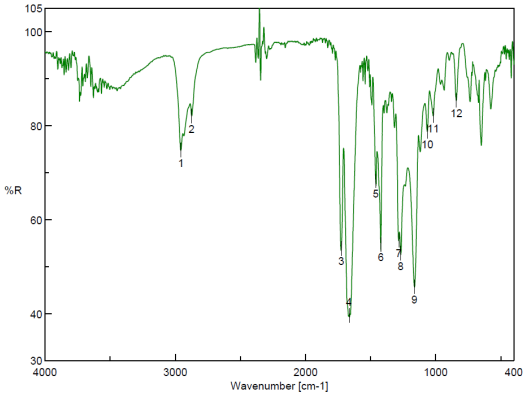

No.	Position	Intensity	No.	Position	Intensity
1	2955.38	74.8274	2	2873.42	82.0439
3	1724.05	53.9029	4	1665.23	39.6135
5	1460.81	68.2495	6	1419.35	54.6811
7	1283.39	55.5691	8	1269.9	52.9014
9	1162.87	45.6707	10	1063.55	78.7611
11	1018.23	82.1636	12	840.812	85.3921

PBMEGMA

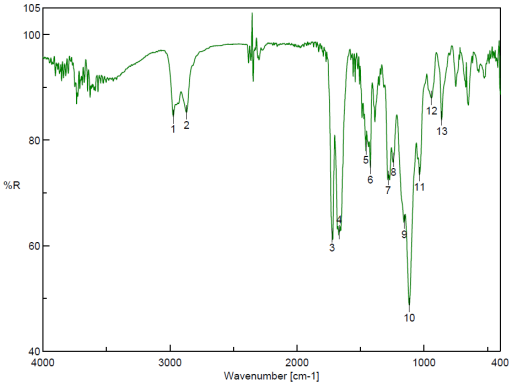

No.	Position	Intensity	No.	Position	Intensity
1	2973.7	84.3919	2	2868.59	85.2355
3	1722.12	61.9407	4	1667.16	62.499
5	1455.99	78.5605	6	1422.24	74.8283
7	1281.47	72.8235	8	1240	76.2636
9	1154.19	64.5351	10	1115.62	48.6958
11	1033.66	73.5054	12	940.128	87.944
13	859.132	84.0655			

PB20_80A1

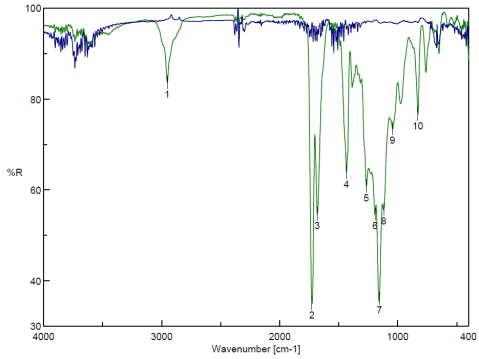

No.	Position	Intensity	No.	Position	Intensity	No.	Position	Intensity
1	2952.48	83.626	2	1725.98	34.9956	3	1680.66	54.7113
4	1433.82	63.8265	5	1265.07	60.8032	6	1190.83	54.6777
7	1154.19	36.0689	8	1117.55	55.6782	9	1045.23	73.5555
10	829.241	76.6755						

PB80_20A4

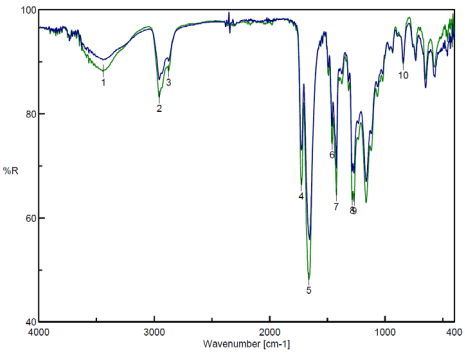

No.	Position	Intensity	No.	Position	Intensity
1	3439.42	88.2386	2	2955.38	83.1964
3	2873.42	88.2268	4	1724.05	66.3231
5	1658.48	48.2449	6	1458.89	74.2668
7	1422.24	64.384	8	1283.39	63.5539
9	1267.97	63.5065	10	842.74	89.6189

PB80_20A1

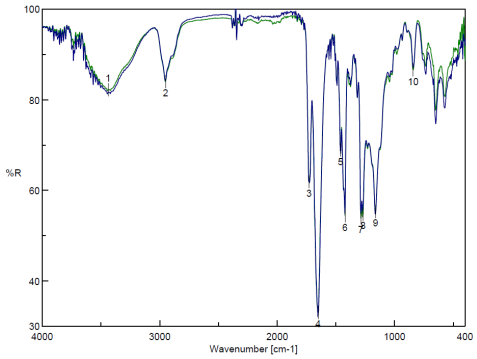

No.	Position	Intensity	No.	Position	Intensity	No.	Position	Intensity
1	3439.42	82.1454	2	2950.55	84.0249	3	1725.98	61.9045
4	1651.73	33.0191	5	1460.81	68.896	6	1422.24	54.3915
7	1286.29	53.8852	8	1267.97	54.7805	9	1160.94	55.3313
10	840.812	86.5778						

PBM2

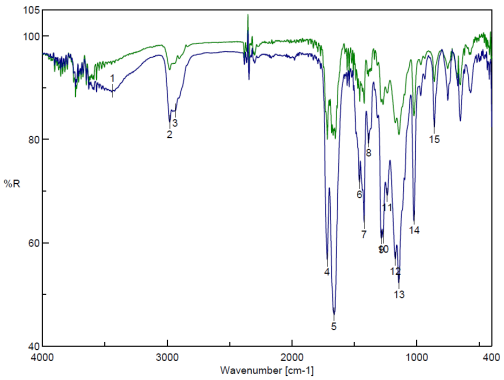

No.	Position	Intensity	No.	Position	Intensity	No.	Position	Intensity
1	3439.42	89.3178	2	2980.45	83.3052	3	2935.13	85.4812
4	1717.3	56.7409	5	1663.3	46.1592	6	1458.89	71.7278
7	1422.24	63.9422	8	1383.68	79.7356	9	1283.39	61.0584
10	1269.9	61.1119	11	1238.08	69.2404	12	1172.51	56.8725
13	1142.62	52.4029	14	1020.16	64.8022	15	859.132	82.3657

JGSA2

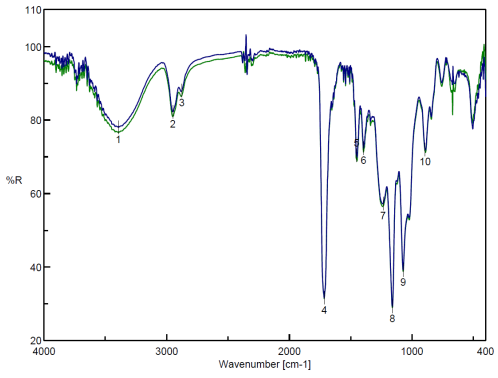

No.	Position	Intensity	No.	Position	Intensity	No.	Position	Intensity
1	3393.14	77.9336	2	2950.55	82.174	3	2875.34	87.9511
4	1715.37	31.6073	5	1451.17	70.3582	6	1395.25	72.3179
7	1236.15	57.1878	8	1159.01	29.2924	9	1072.23	39.1788
10	892.88	71.9454						

Figure S6. IR spectra of studied polymers. Green spectra: pristine polymers. Blue spectra: polymers after being in the presence of $PdCl_2$·NaCl, 5 mM solution.

There was no difference in the IR after being in the presence of Pd(II) solution. With the exception of PB20_80A1 that, because of the presence of Pd(0) nanoparticles, the IR absorption highly decreased.

SEM and EDX analysis:

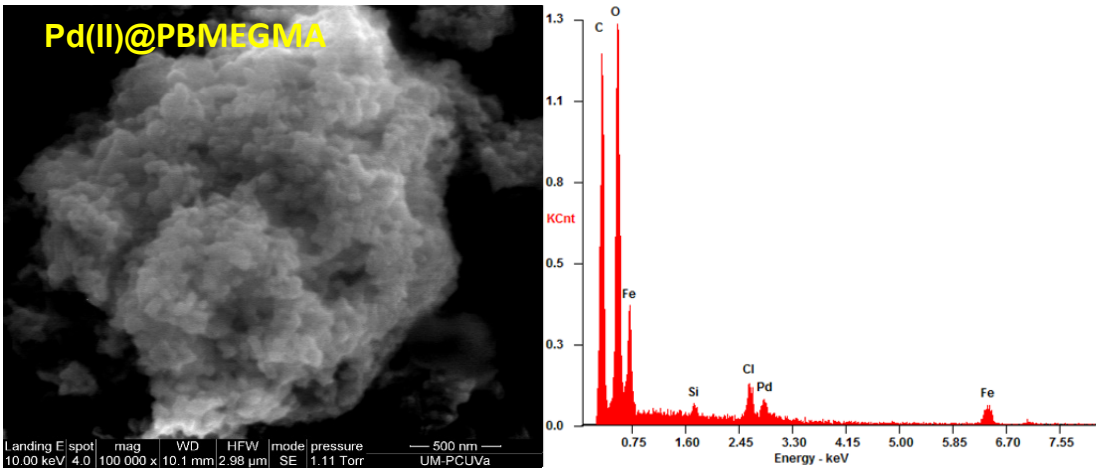

Figure S7. SEM image of Pd(II)@PBMEGMA (left). EDX analysis (right). 1 µm aggregates of $PdCl_2$.

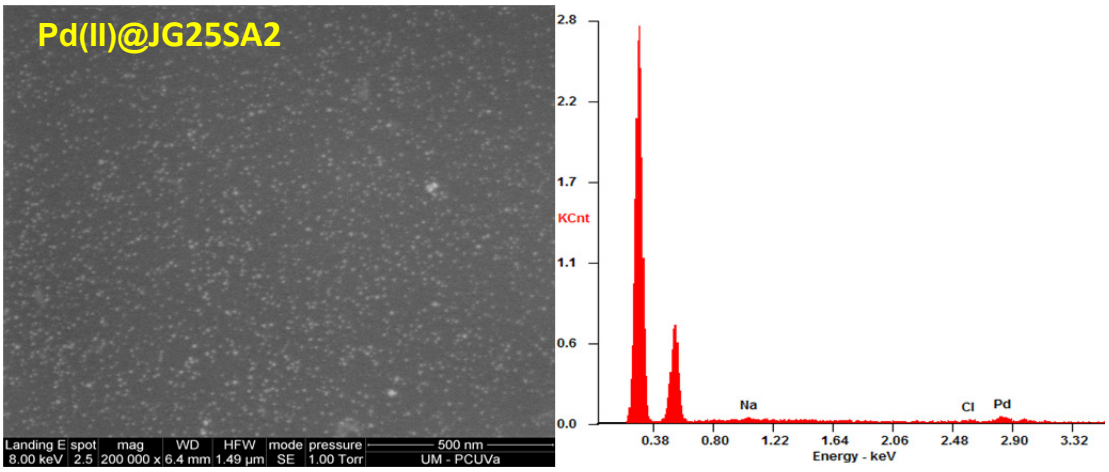

Figure S8. SEM image of Pd(II)@JGSA2 (left). EDX analysis (right). 20 nm aggregates of $PdCl_2$.

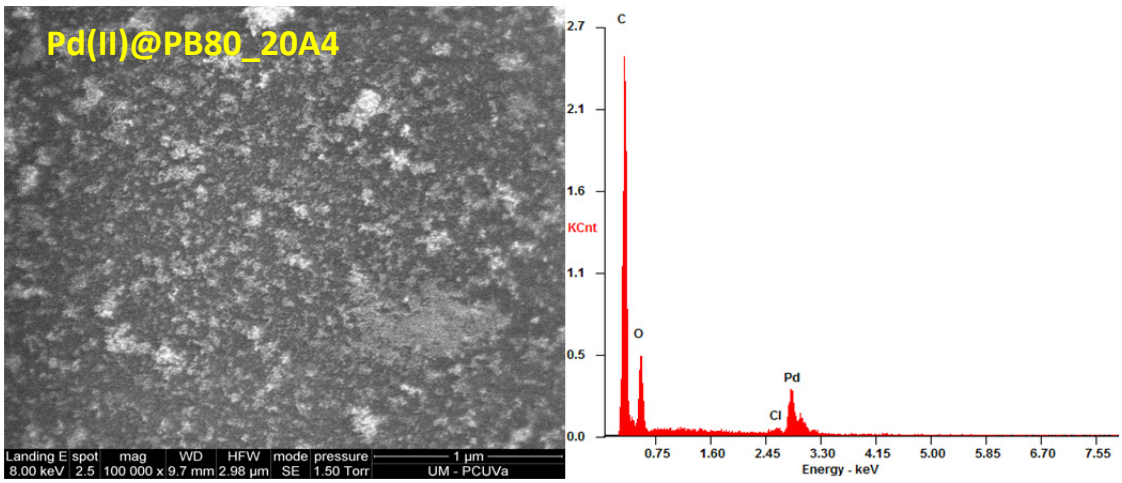

Figure S9. SEM image of Pd(II)@PB80_20A4 (left). EDX analysis (right). 20 nm aggregates of $PdCl_2$ and Pd(0).

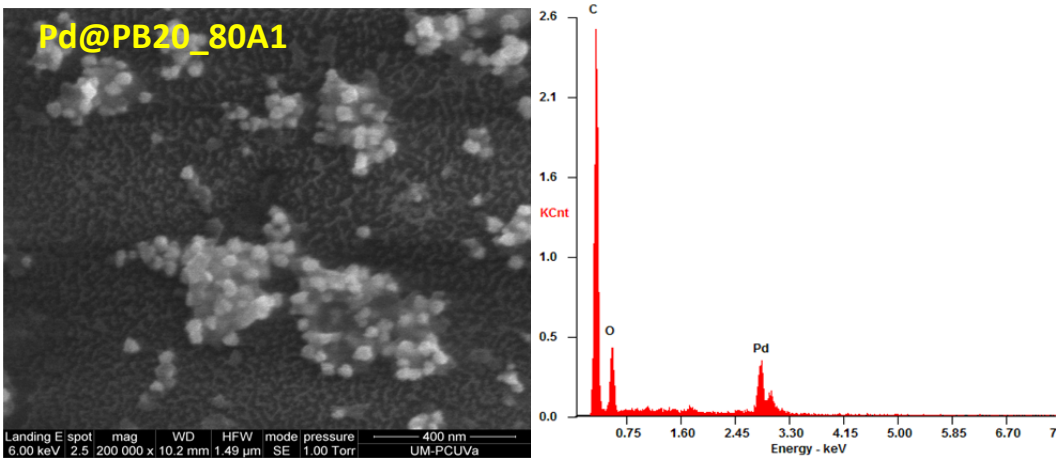

Figure S10. SEM image of Pd@PB20_80A1 (left). EDX analysis (right). Aggregated NPs of Pd(0).

Different aggregates were observed depending on the polymer. Moreover, from the EDX, it was obtained that some aggregates are Pd(II), or mixtures Pd(0) + Pd(II), in those cases containing chloride anion, in all cases except Pd@PB20_80A1 in which there was no chloride anion.

XPS Characterization:

The three samples with better performance for different applications were also analysed by **XPS:**

In the analysis it is shown the signal under different voltages. One peak is associated to the presence of Pd(II) and the other to Pd(0). In addition to the results from EDX, previously shown, it provides an estimation of the presence of each one of them.

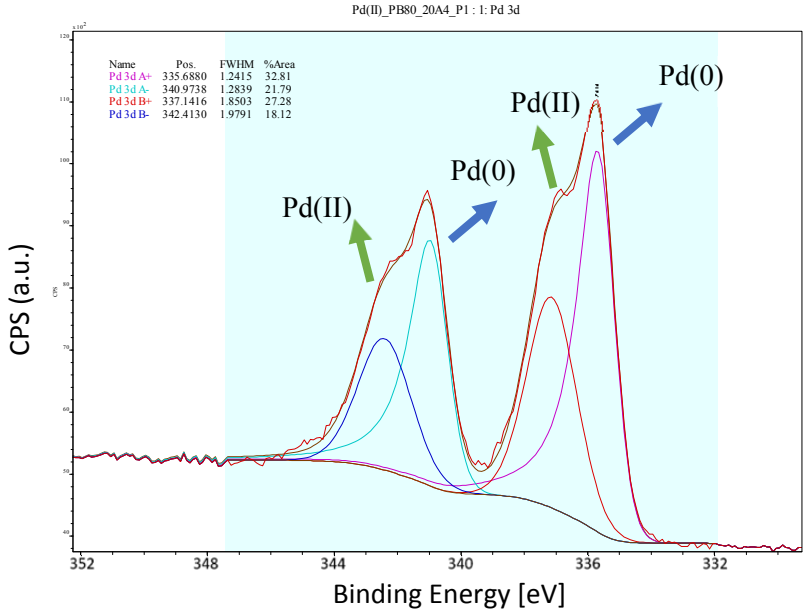

Figure S11. XPS Analysis of Pd(II)@PB80_20A4, the proportions where a 45:55 for Pd(II):Pd(0).

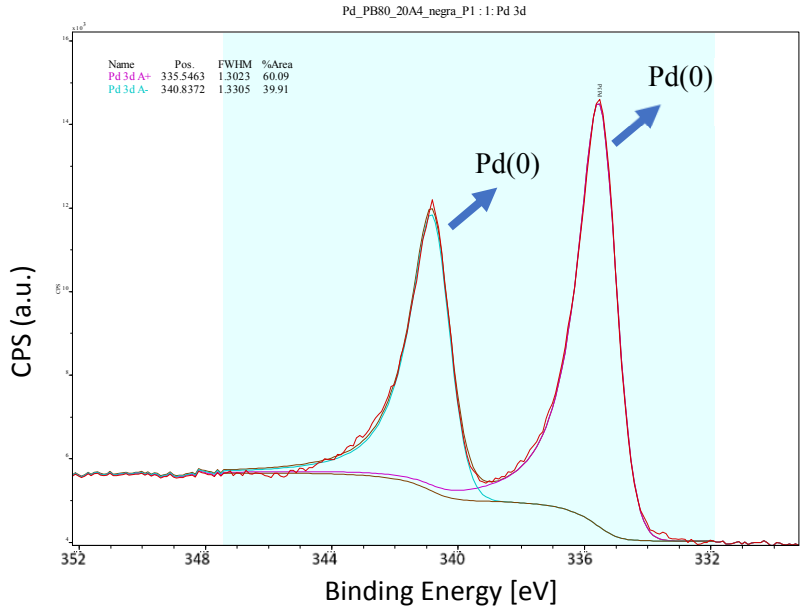

Figure S12. XPS Analysis of Pd@PB80_20A4 being a 100 % Pd(0).

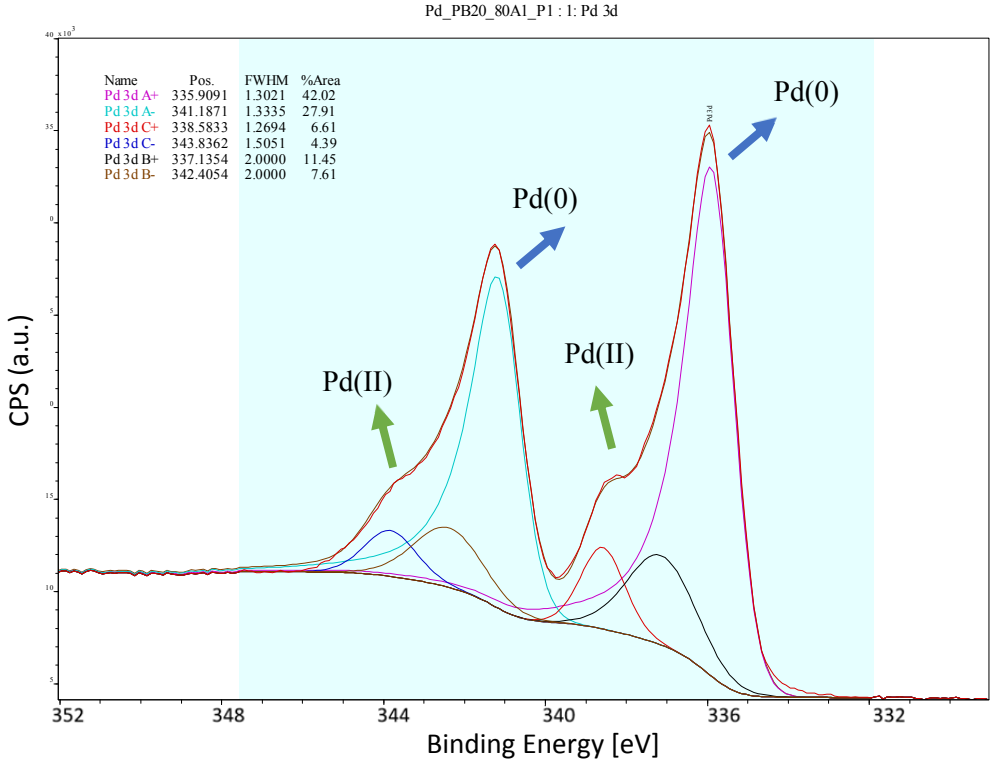

Figure S13. XPS Analysis of Pd@PB20_80A1, the proportions where a 20:80 for Pd(II):Pd(0).

The presence of Pd(II) in Pd@PB20_80A1 was a consequence of the lack of washing procedure of the polymer (due to the possibility of losing the deposited nanoparticles. Additionally, if the results of the EDX are taken into account (which gives the composition with more deepness) it is not detected apart from a very low amount in the surface.

UV-Vis absorption spectra:

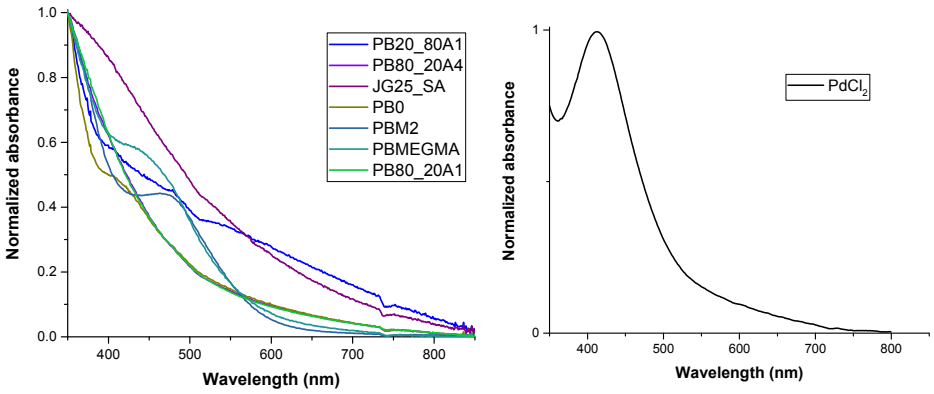

Figure S14. Normalized Absorption spectra of differently synthesized polymers (left) and $PdCl_2$·2NaCl 5mM solution in water (right).

The colour or UV-vis absorption is a way to characterize the formation of Pd(0), by comparison with the results from literature.[1] $PdCl_4^{2+}$ in water solution has a yellow-orange colour with a characteristic absorption at 420 nm, as it can be seen in Figure S11. In contrast, Pd(0) particles lead to the disappearance of this band, getting a wider absorption that decays continuously from 350 nm to 850 nm.

The results of the tests led to different absorption values depending on the polymer. In conclusion, high absorbances at 400-500 nm indicated the presence of starting $PdCl_4^{2+}$, clearly showed in PB0, PBMEGMA and PBM2. However, other films are more difficult to distinguish, such as PB80_20 or JG25_SA, that needed for verification some other techniques.

Loadings of the polymers.

Two samples of the polymers with better results (around 8 milligrams each) were weighed before and after react with the Pd(II) salt in solution.

	Initial/Final weight		% weight increase
PB20_80A1	0.0146	0.0132	1.13
	0.0115	0.00914	
	0.00984	0.0095	
PB80_20A4	0.0241	0.0211	2.35
	0.0268	0.0226	
	0.0231	0.0231	

Figure S15. Loadings of PB20_80A1 and PB80_20A4

The increase in weight was around 1.1-2.4 %. In case of PB20_80A1, the repeatability was lower because of the transferable particles.

Other studies and characteristics:

Apart from the characteristics showed for selected polymers in previous characterization methods, there are some polymers that had some other remarkable behaviours:

1) **Pd@PB20_80A1** presented transferable Pd nanoparticles agglomerates on its surface, which is explained in the main paper

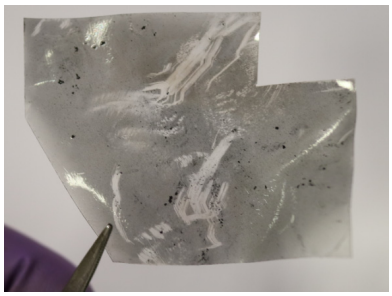

Figure S16. General picture of the polymer Pd@PB20_80A1.

2) **PB80_20A4 (or PB80_20A1)** can be reduced under H_2 atmosphere.

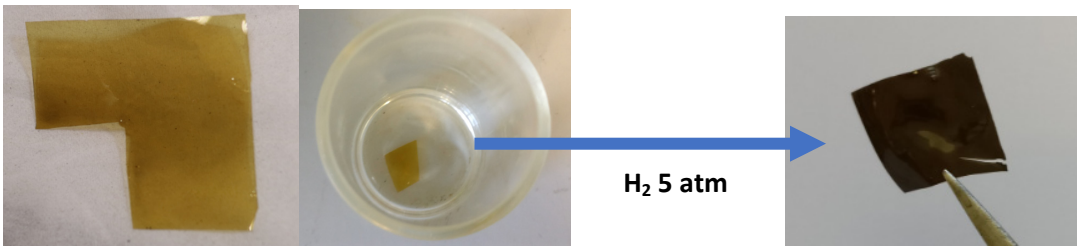

Figure S17. Pd(II)@PB80_20A4 after being in presence of $PdCl_2$·2NaCl solution in water (left) and after placing this polymer under H_2 atmosphere to get Pd@PB80_20A4 (right).

2. Pd SUPPORTED POLYMERS AS CATALYSTS

After the development of different surfaces modified with Pd particles, the next objective was to use them as palladium catalysts for semihydrogenation reductions of alkynes to *Z*-alkenes.

To have the best conditions as heterogenous catalyst the next characteristics must be fulfilled:

- Using green solvents (avoiding DCM or DMSO).
- High reusability of the catalysts.
- No leaching of Pd to the solutions.
- The ratio [Pd (mol)]/Polymer surface (cm^2) has to be as low as possible.
- The turnover number (TON), (number of moles converted to product)/(surface of the heterogeneous catalyst), has to be as high as possible.

From all the polymers that contained palladium in its surface the most stable were selected:

- PB20_80A1. That gave Pd nanoparticles transferable to other surfaces.
- PB80_20A1 or A4. With previously reduced Pd nanoparticles.
- JG25SA, which was, apparently, very similar to PB80_20.

There were several examples of supported catalysts for the reduction of triple bonds. The most common are Pd/C (alkynes to alkanes) and Lindlar catalyst (falkynes to *Z*-alkenes) which are widely used but also very expensive. These catalysts have some issues such as requiring a filtration, the need for great amounts of the catalysts or low (if some) reusability. As a consequence, it was of upmost importance the development of new catalysts that overcome those problems.

- The **solvent** had to be valid for most organic compounds. With that purpose, the reaction was tested in MeOH (most common and capable to dissolve organic compounds), DCM and THF.
- The film was **0.5×0.5 cm for 5 mL solution**.
- The selected sample for reduction was **dimethyl acetylenedicarboxylate (DMAD)**, that was added as much as 500 mg in 5 mL. To test the capabilities of the polymer as a catalyst, dimethyl acetylenedicarboxylate is interesting for several reasons:
    - It is soluble in common solvents, such as methanol or dichloromethane.
    - It is simple to analyze, is liquid and there is only one signal in the ^{1}HNMR spectra.

- It does not have an isolated triple bond, that is conjugated with the ester groups, however it is not a large conjugation. This means that the reaction wouldn't be totally favored nor disfavored.

Starting material, expected products in ^{1}HNMR.

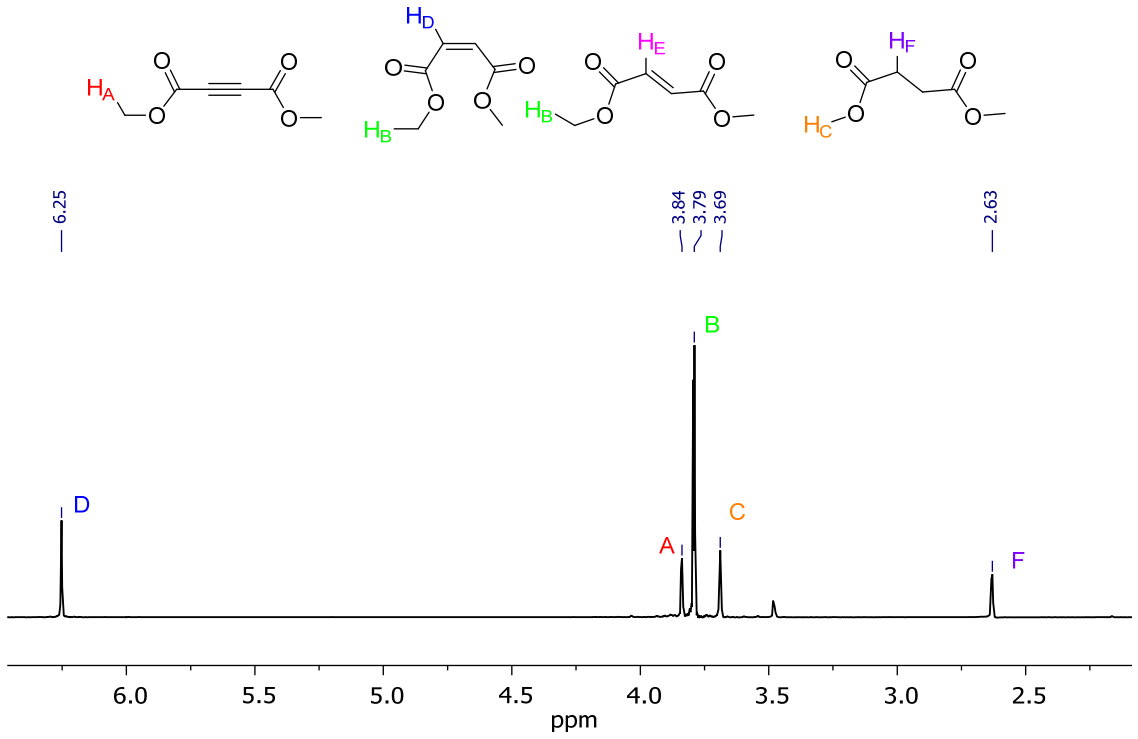

Figure S18. Possible products of the reduction of the triple bond from DMAD (up) and ^{1}HNMR spectrum obtained from using the polymer as catalyst (down). The film used for the example was Pd(II)@PB20_80A4, without previous cleaning nor reduction.

In ^{1}HNMR from the **Figure S18** it can be seen the presence of a mixture between the starting material, dimethyl maleate and the all reduced dimethyl succinate. Dimethyl fumarate was rarely obtained (THF solutions) and in very low yields. As a result, all the products expected may be easily detected by ^{1}HNMR, the only one that was obtained in very low quantities was the dimethyl fumarate (Yield < 10%).

Specific conditions for the tests:

In 10 mL vials, 500 mg of dimethyl acetylenedicarboxylate were dissolved in 5 mL of the chosen solvent. Afterwards, a piece of polymer, 0.5×0.5 cm, was added to the solution.

The vial was put in a reactor and H_2 was introduced to the chamber until reaching 5 atm, the polymer remained under H_2 atm for 13-16 hours.

Reduction of DMAD with Pd supported films:

The following table summarizes the results:

Polymer	Solvent	Initial (%)	Cis (%)	Trans (%)	Simple (%)
No catalyst	-	100	0	0	0
	MeOH	97	<3	0	0
	DCM	100	0	0	0
	THF	100	0	0	0
PB80_20A4*	-	93	7	0	0
	MeOH	10	90	0	0
	DCM	26	74	0	0
	THF	37	46	9	8
PB20_80A1	-	90	10	0	0
	MeOH	6	94	0	0
	DCM	71	29	0	0
	THF	83	8	9	0
JG25SA2	-	93	7	0	0
	MeOH	56	40	0	4
	DCM	97	3	0	0
	THF	9	8	6	0

*PB80_20A4 palladium was previously reduced under H_2 atmosphere 5 atm, 1 hour and washed 5 times with 10 mL of MeOH.

Figure S19. Reduction of the triple bond from DMAD in presence of three different heterogenous catalysts, three different solvents and with no solvent.

Previously to give an analysis of the results, there are several considerations to take into account:

- **Best yields** (% reacted) were reached for PB20_80A1 and PB80_20A4 by using MeOH as solvent. In addition, the yields of several repetitions are shown in the following table.

	Polymer	Initial (%)	Cis(%)	Simple(%)
1st	**Pd(II)@PB80_20A4***	5	72	23
	Pd@PB20_80A1	6	94	0
2nd	**Pd@PB80_20A4***	9	85	6
	Pd@PB20_80A1	21	79	0
3rd	**Pd@PB80_20A4**	5	95	0
	Pd@PB20_80A1	32	68	0
4th	**Pd@PB80_20A4**	8	92	0
	Pd@PB20_80A1	65	35	0

*The polymer was not previously reduced and washed before the reactions. If done so, the yields are similar to the reactions done afterwards.

Figure S20. Reduction of the triple bond from DMAD in presence of 3 different heterogenous catalysts, 3 different solvents and without solvent.

- Pd@PB20_80A1 has the drawback (for catalytic purposes) of the transferable particles, if the polymer was scratched, or put in contact with some surfaces, the quantity of particles decreases. Also, there could be transference to the solutions (although is not soluble in MeOH) loosing effectiveness and reducing the reusability.

- Pd(II)@PB80_20A4 has the simple bond (succinate) as a by-product in the first two reactions. This is the consequence of using the not reduced-not washed polymer. After the second reaction, it is constant at least for 4 reactions more with yields of the cis product (maleate) superior 90 %.

- Pd@PB80_20A4 has the best yield/reusability but, in order to have no by-products, such as the simple bond, the polymer should be carefully washed with MeOH, and previously subjected to hydrogen atmosphere. As a result, it can be used as a catalyst with very high yields.

- Other molecules reach quantitative yields (>99%) with the same solvents (see section 3, “catalytic reduction of compounds with biological interest”). The yield varies depending on the solvents and the molecule to be reduced (the surroundings of the triple bond), apart from being limited by its TON.

- Pd(II)JG25SA2 gave similar results to PB80_20A4, but a much worse yield. Additionally, the mechanical properties were much worse; therefore, it was not further studied.

- In comparison with Lindlar catalyst (**Figure S21**), the results were more selective and, especially in MeOH, Lindlar catalyst had tendency to lead to a more "reduced" product (succinate derivative) depending on the conditions. (50 mg of catalyst, same conditions).

	DMAD + Lindlar catalyst		
	MeOH	**THF**	**THF+Quinoline**
***Z*-reduced**	0	71	80
Alkyne to alkane	100	29	20

Figure S21. Products of hydrogenation reactions of DMAD in MeOH, THF and THF+Quinoline with Lindlar catalyst in THF+Quinoline.

Leaching of the polymers:

One of the biggest issues of using Pd supported catalysts is the quantity of the palladium that leaks to the solution. Several situations were studied, to do so an aliquot of the solution from the reaction (1 mL) was analyzed by ICP mass (three times each) and calibrated with palladium solutions. The results were:

- PB20_80A1: the palladium in solution is negligible, due to the insolubility and despite the being transferable. The quantity detected was lower to 2 µM.
- PB80_20A4 before reducing and washing the polymer: the quantity detected was between 0.4 to 0.1 mM.
- PB80_20A4 after reducing and washing the polymer: The quantity detected was lower to 6 µM.

These data are also important in order to show the necessity of using washed polymers. Furthermore, this shows the influence of the presence of non-reduced Pd, which leads to obtain products reduced to simple bond, which does not occur when using the reduced ones.

Other important characteristics studied:

- *Reaction time:* the reaction time was tested in MeOH solution. The yield was the same between 5 to 72 hours. However, less time led to lower yields, although this parameter should be adjusted depending on the

specific molecule to reduce, and also depends on other parameters like concentration or temperature

- *Polymers without crosslinker:* PBM2, PBMEGMA and PBMA didn't have crosslinker, that caused that they were soluble in most of the organic solvents. Despite this fact, they were tested in solution but the reaction didn't work.
- *Turnover number (TON):* in this case TON was defined as product moles/surface, and it was calculated based on the studied reduction reaction. In this regard, the catalyst turnover number was calculated, by considering a yield of 90% in previous reactions, for the cis product, 75 mmoles/cm^2.

3. CATALYTIC REDUCTION OF COMPOUNDS WITH PHARMACOLOGICAL INTEREST

With the polymer with the best results (Pd@PB80_20A4) and the optimized conditions, a series of compounds were selected on the basis of their special properties and applications in different fields such as medical drugs:

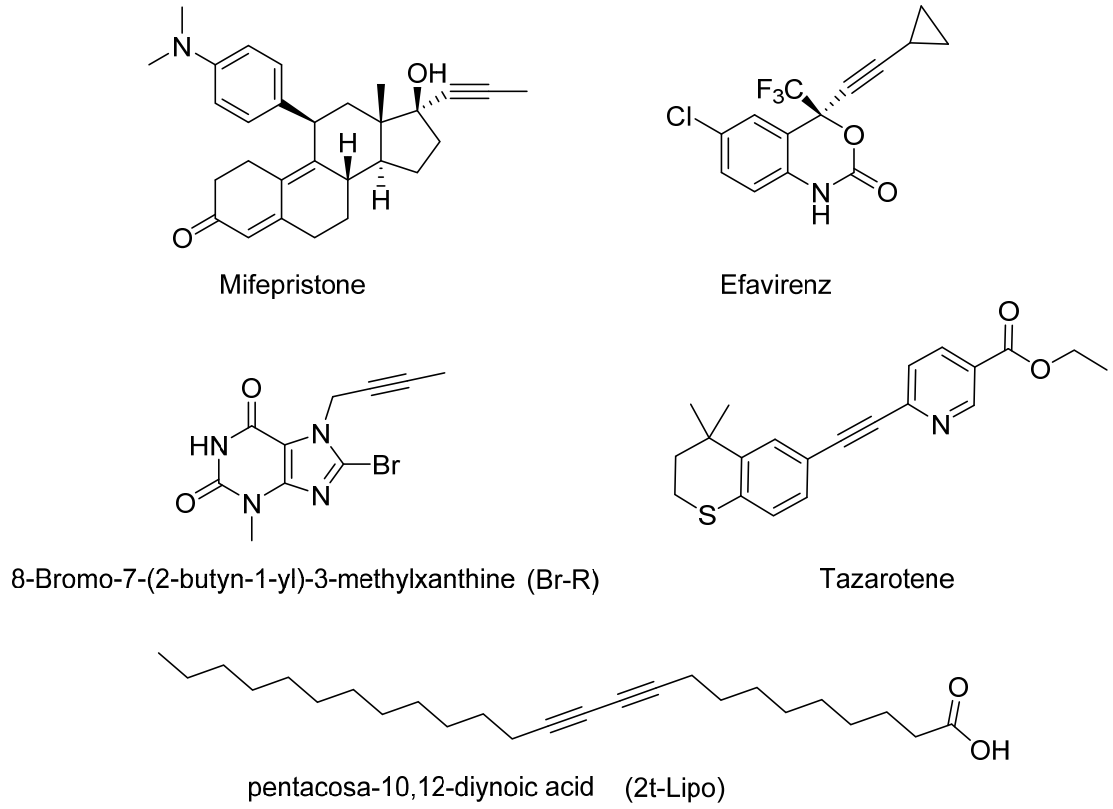

Figure S22. Molecules with triple bonds studied

In addition to the use of this new heterogeneous catalyst, the results were compared, by using the classic Pd/C (10%) catalyst in the reaction and using Lindlar catalyst.

Conditions of the reaction and yields obtained:

The reaction conditions are similar to the DMAD reduction. 50-100 mg of the molecules were dissolved in 2-5 mL of MeOH and placed under 5 atm of H_2.

Yields obtained for the cis product:

Pd@PB80_20A4	cis (%)
Efavirenz	>99
Mifepristone	>99
Br-R	90
Tazarotene	85
2t-Lipo*	≥50

Figure S23. Yields (%) of the cis product.

These yields were calculated after the purification by column chromatography of the product except for 2t-Lipo. Characteristics of each reaction:

- *Efavirenz and Mifepristone* had a favoured reduction reaction, with yields higher to 99 % and without by-products.
- *Br-R* had several minor by-products, needing column chromatography for the separation of the cis product.
- *Tazarotene* was less reactive under the same reaction conditions, therefore, an easy separation from the remaining starting material, that was reused, was also needed.
- *2t-Lipo* was only slightly soluble in MeOH and chloroform. Nevertheless, the reaction occurs with high yields as it can be deduced from ^{1}H NMR, which demonstrated its applicability for the purpose of reducing triple bonds in lipidic chains. In this case, the yield was estimated from the ^{1}H NMR because a column chromatography was not possible due to its low solubility in the common solvents.

Comparison with Pd/C catalyst:

The importance of using this catalyst may be seen by comparing previous results with the results by using commercial Pd/C (10%). In this way, the reaction was performed with this classical catalyst under similar conditions: 100 mg of efavirenz, 5 mL of MeOH, 100 mg of Pd/C at 5 atm for 16 hours.

Efavirenz:

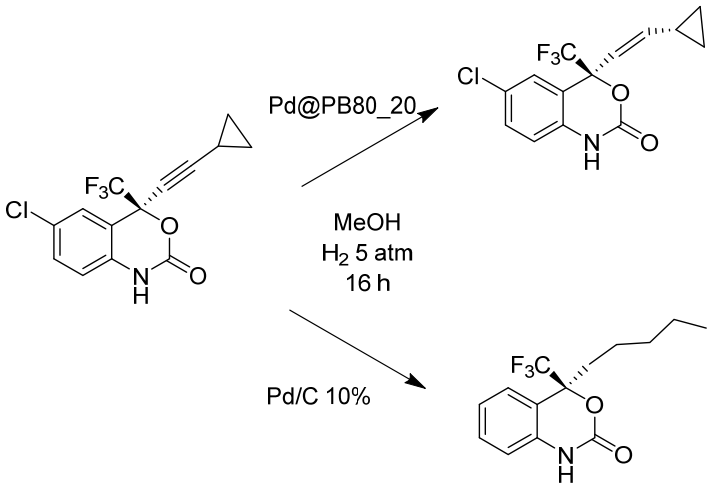

Figure S24. Efavirenz reduction.

The reaction with Pd/C leads to the reduction of the triple bond to simple bond and the dehalogenation of the aryl-chloride. The product was obtained in quantitative yield.

Mifepristone:

In this case, the product obtained under Pd/C catalysis was a mixture of different reduction products, as it was checked by mass spectrometry (See the characterization section in page S27). Apparently, the starting material underwent reduction in more than one different position, due to the presence of double bonds in its structure.

Br-R:

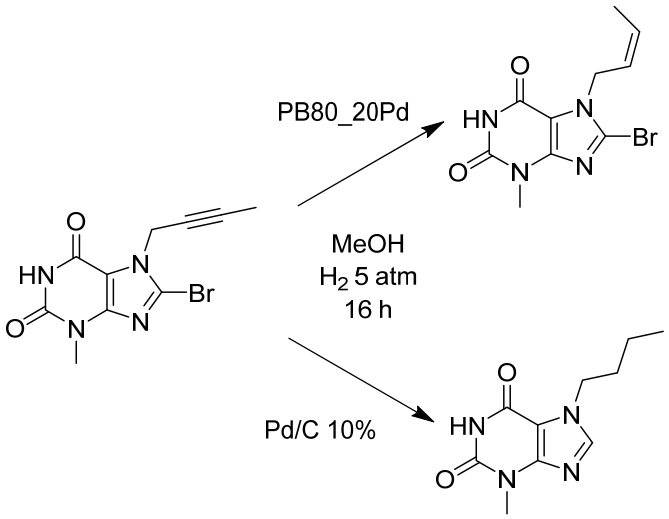

Figure S25. Br-R reduction scheme.

Just as Efavirenz, the reaction with Pd/C leads to the reduction of the triple bond to simple bond and the dehalogenation of the aryl bromide. The product was obtained in quantitative yield.

Tazarotene:

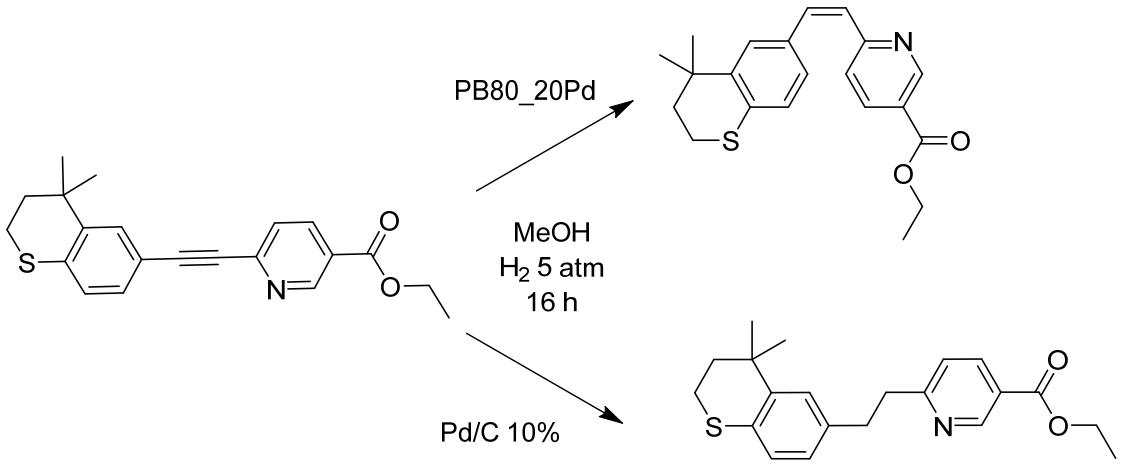

Figure S26. Tazarotene reduction scheme.

The reaction with Pd/C leads to the reduction of the triple bond to simple bond. The product was obtained in quantitative yield.

Characterization of the products:

The products can be easily distinguished from the starting material by ^{1}HNMR spectroscopy. Apart from this, HRMS, full ^{1}HNMR, ^{19}FNMR and ^{13}CNMR are provided.

Efavirenz derivatives:

a) Comparison starting material – Pd@polymer reduction:

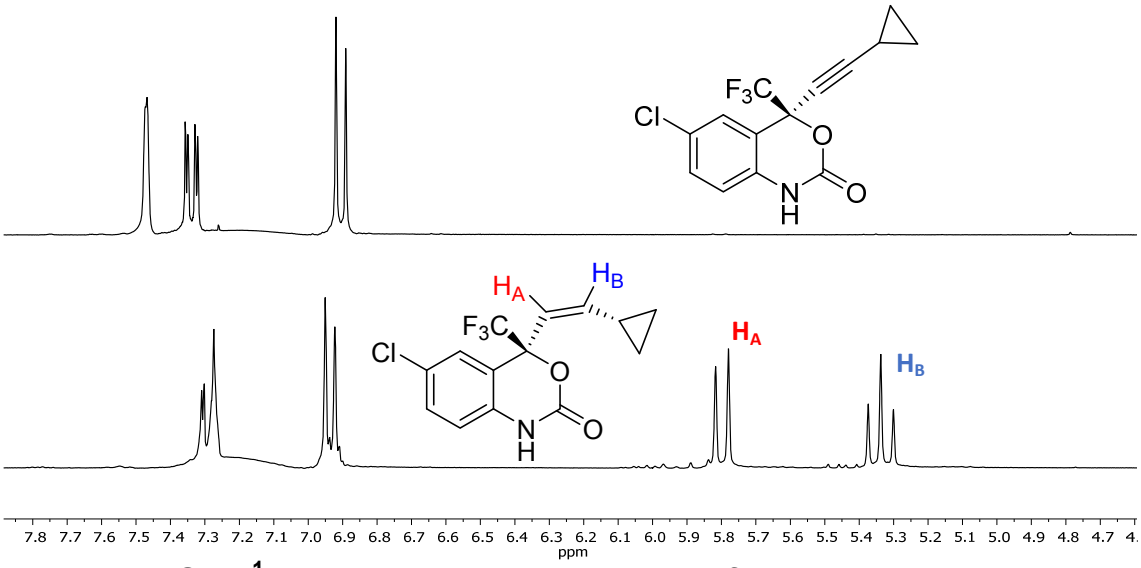

Figure S27. ^{1}H NMR comparison between Efavirenz and Z-dihydro Efavirenz, its cis-reduced species.

b) Pd@polymer reduced Efavirenz characterization:

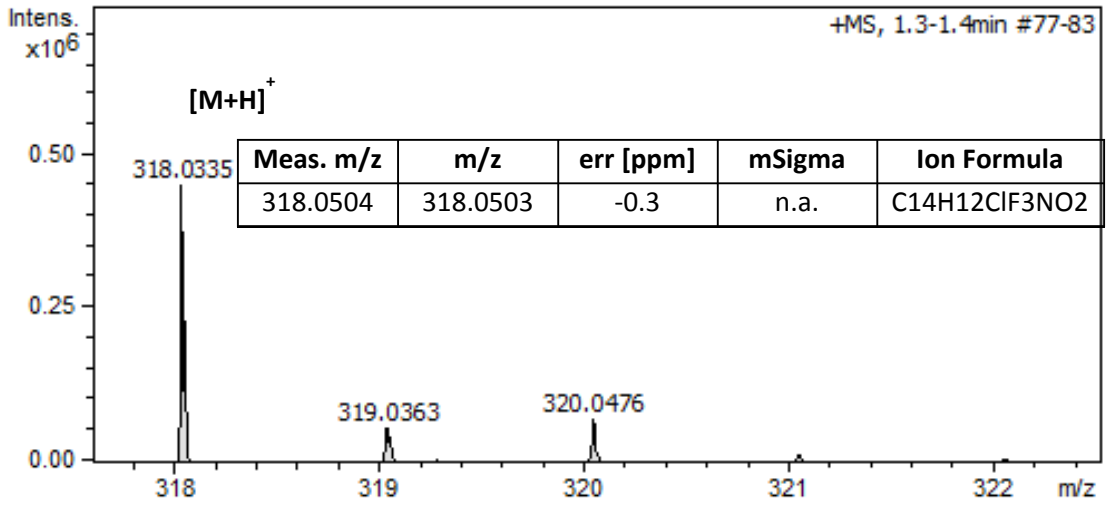

Meas. m/z	m/z	err [ppm]	mSigma	Ion Formula
318.0504	318.0503	-0.3	n.a.	C14H12ClF3NO2

Figure S28. Mass spectra of Z-dihydro Efavirenz.

HRMS (ESI-TOF) m/z calcd for $C_{34}H_{29}NO_2$ (M^+): 483.2193; found: 483.2224.

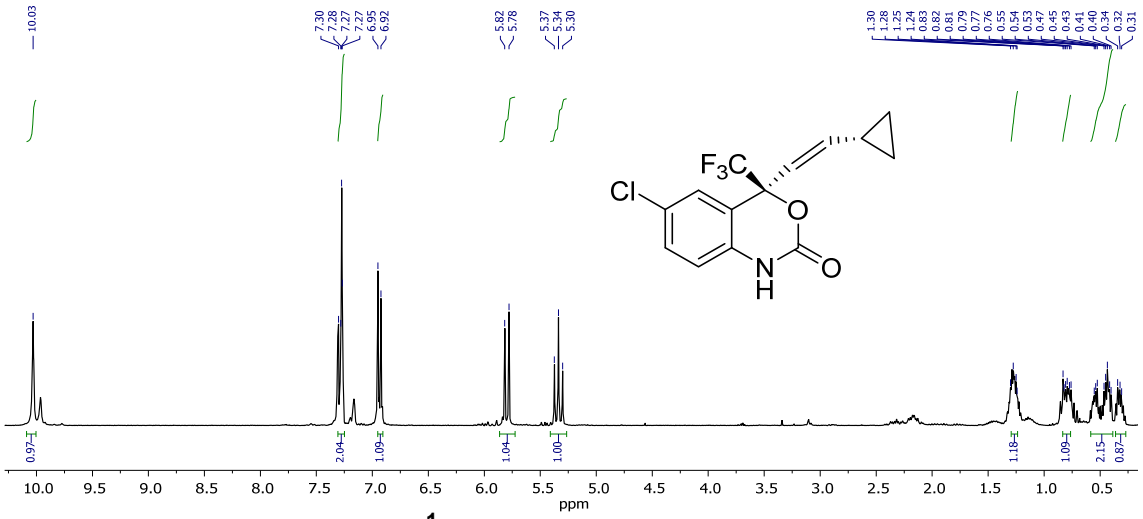

Figure S29. ^{1}H NMR of Z-dihydro Efavirenz.

^{1}H NMR (300 MHz, $CDCl_3$) δ 10.03 (s, 1H, NH), 730-7.27 (m, 2H, H_{Ar}), 6.94 (d, *J = 8.3 Hz*, 1H, H_{Ar}), 5.80 (d, *J = 11.2 Hz*, 1H, C=CH), 5.34 (t, *J = 11.0 Hz*, 1H, C=CH), 1.27 (m, 1H, CH), 0.81 (m, 1H, CH_2), 0.55-0.30 (m, 3H, CH_2).

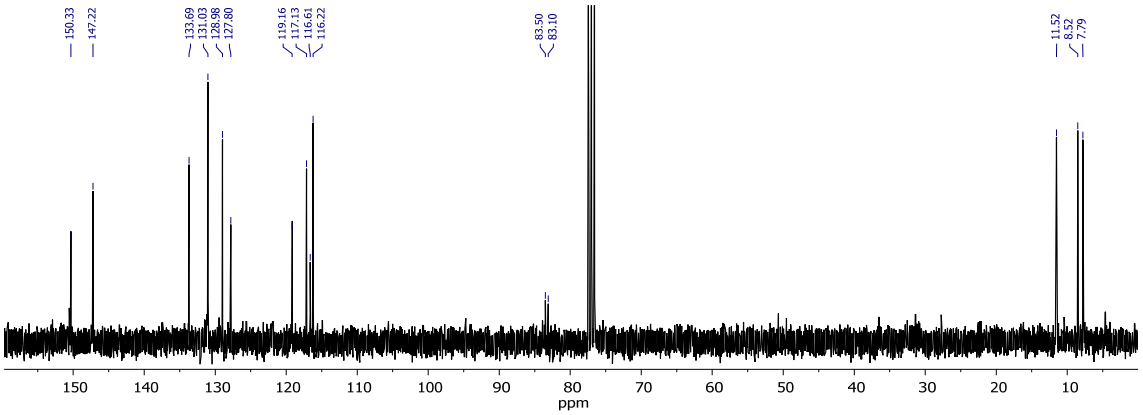

Figure S30. ^{13}C NMR of Z-dihydro Efavirenz.

^{13}C NMR (75 MHz, $CDCl_3$) δ 150.33 (C=O), 147.22 (CH=**C**H-CH), 133.69 (C-NH), 131.03 (CH), 128.98 (C-Cl), 127.80 (C-Cl), 119.16 (CH), 117.13 (CF_3), 116.61 (CH), 116.22 (CH), 83.5-83.1 (**C**-CF_3), 11.52 (**C**H=CH-CH), 8.52 (CH_2), 7.79 (CH_2).

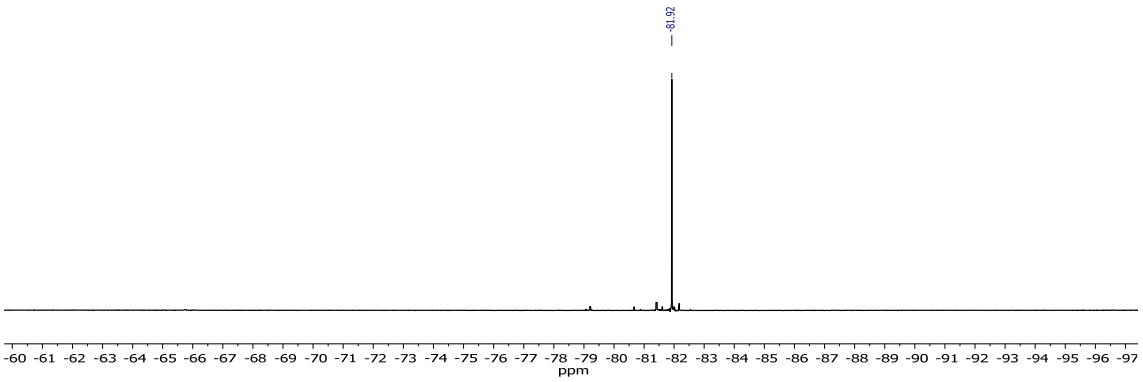

Figure S31. ^{13}CNMR of Z-dihydro Efavirenz.

^{19}F NMR (282 MHz, $CDCl_3$) δ -81.92.

c) <u>Pd/C reduced efavirenz characterization:</u>

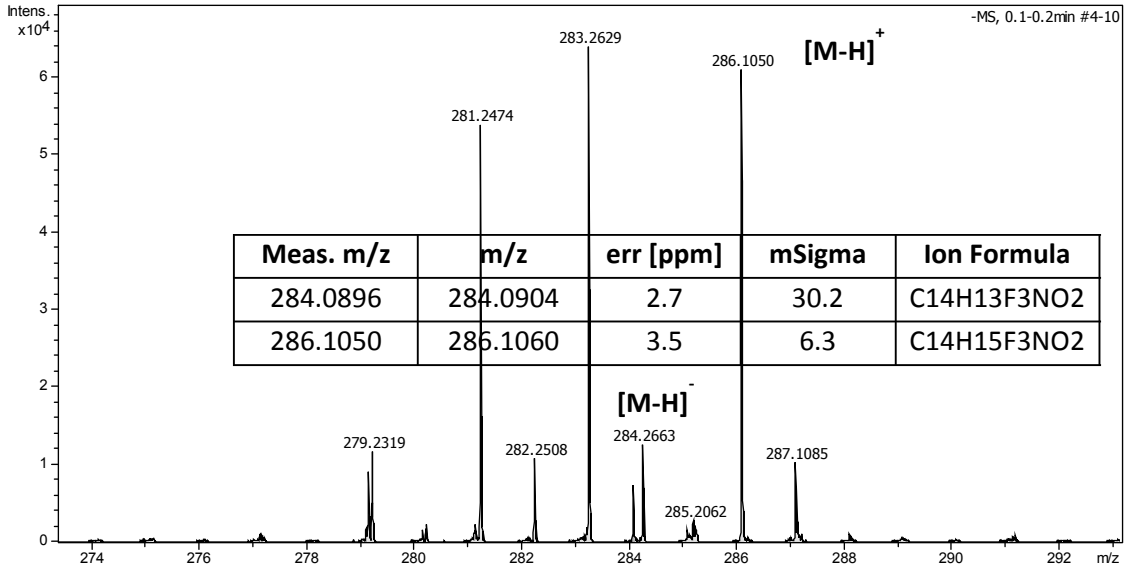

Meas. m/z	m/z	err [ppm]	mSigma	Ion Formula
284.0896	284.0904	2.7	30.2	C14H13F3NO2
286.1050	286.1060	3.5	6.3	C14H15F3NO2

Figure S32. Mass spectra of Pd/C reduced Efavirenz.

HRMS (ESI-TOF) m/z calcd for $C_{14}H_{13}F_3NO_2$ (M^+): 284.0904; found: 284.0896.

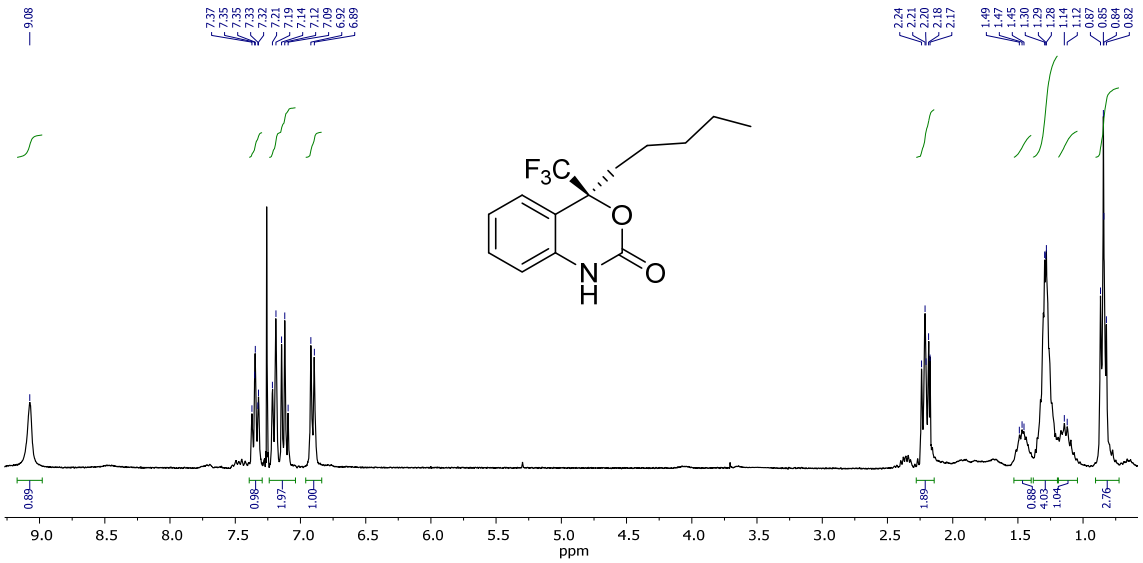

Figure S33. ^{1}H NMR of Pd/C reduced Efavirenz.

^{1}H NMR (300 MHz, $CDCl_3$) δ 9.08 (s, 1H, NH), 7.35 (dd, *J* = 8.3, 6.8 Hz, 1H, CH_{Ar}), 7.24 – 7.02 (m, 2H, CH_{Ar}), 6.91 (d, *J* = 7.9 Hz, 1H, CH_{Ar}), 2.24 – 2.17 (m, 2H, CH_2), 1.49 – 1.45 (m, 1H, CH_2), 1.34 – 1.28 (m, 4H), 1.17 - 1.12 (d, *J* = 6.7 Hz, 1H, CH_2), 0.87 – 0.82 (m, 3H, CH_3).

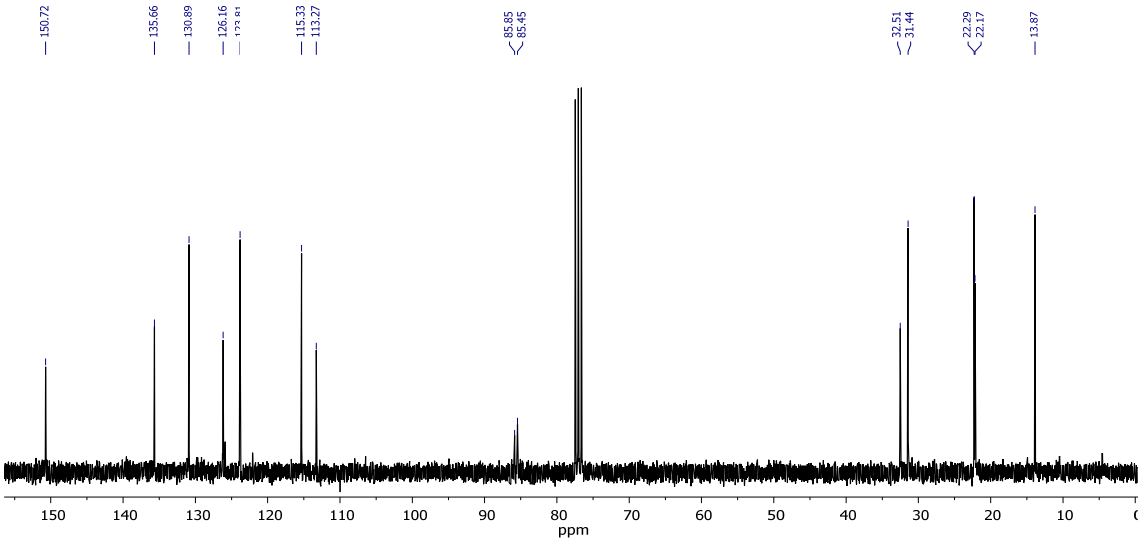

Figure S34. ^{13}C NMR of Pd/C reduced Efavirenz.

^{13}C NMR (75 MHz, $CDCl_3$) δ 150.72 (C=O), 135.66 (C-NH), 130.89 (CH), 126.16 (CH), 123.81 (CH), 115.33 (CH), 113.27 (CF_3), 8.9-85.5 (**C**-CF_3), 32.51 (CH_2), 31.44 (CH_2), 22.29 (CH_2), 22.17 (CH_2), 13.87 (CH_3).

Mifepristone derivatives:

a) Comparison starting material – Pd@polymer reduction:

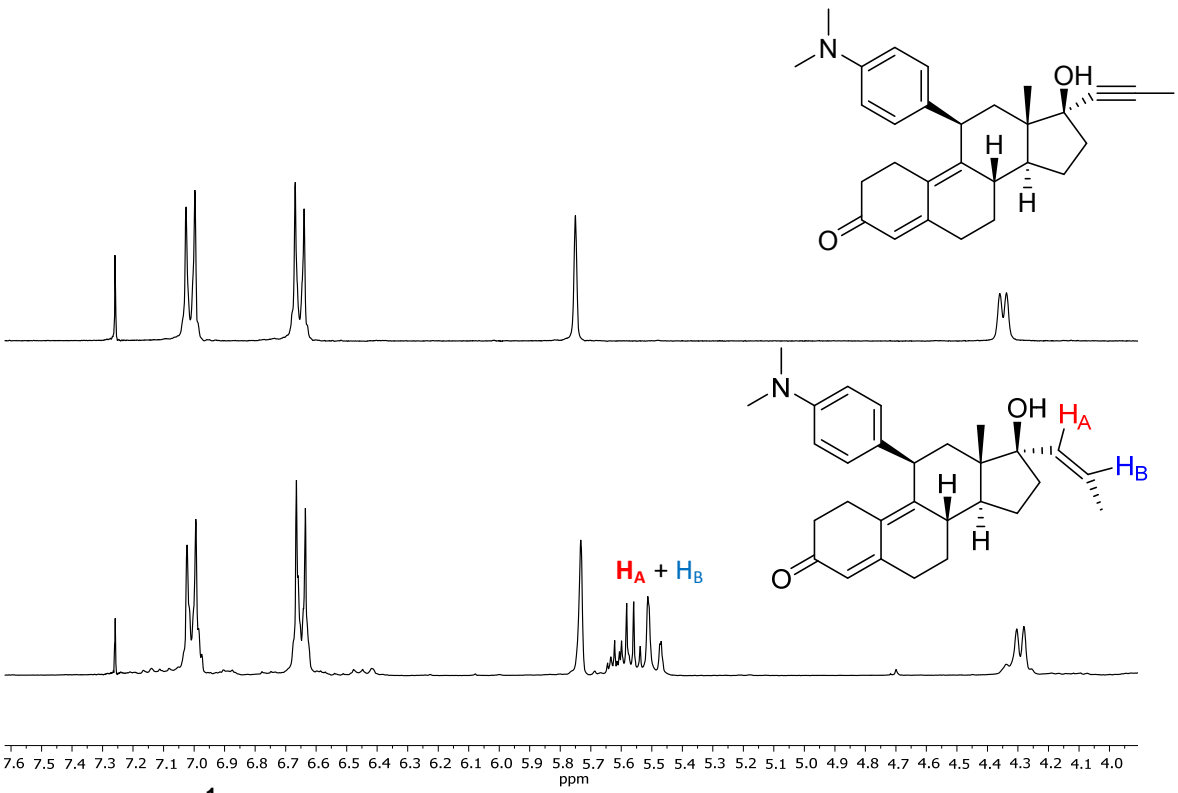

Figure S35. ^{1}H NMR comparison between Mifepristone and Aglepristone.

b) Aglepristone characterization:

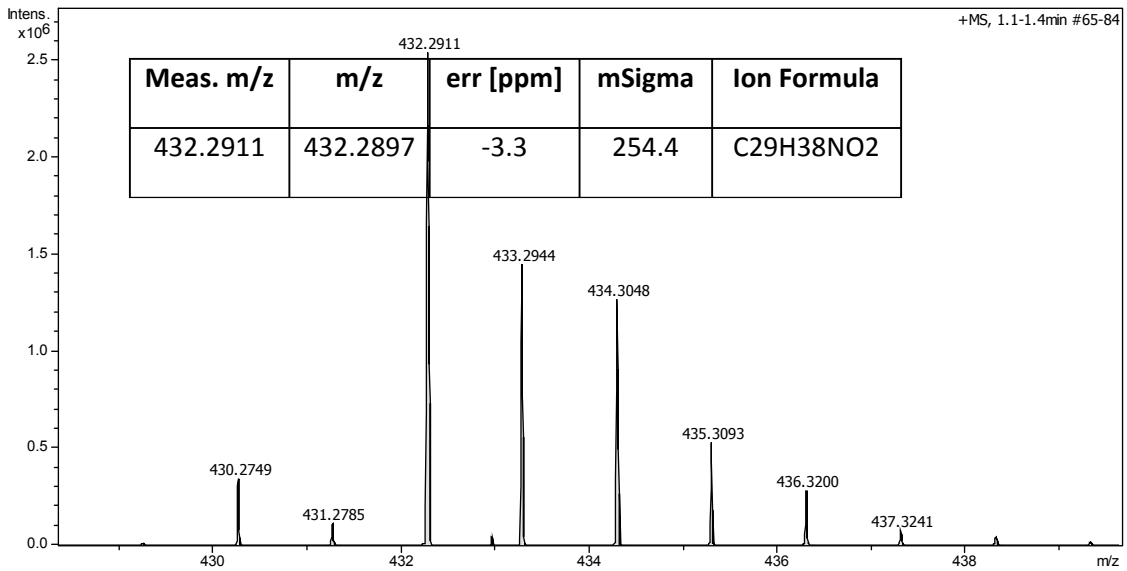

Meas. m/z	m/z	err [ppm]	mSigma	Ion Formula
432.2911	432.2897	-3.3	254.4	C29H38NO2

Figure S36. Mass spectra of cis Reduced Mifepristone.

HRMS (ESI-TOF) m/z calcd for $C_{29}H_{38}NO_2$ (M^+): 432.2897; found: 432.2911.

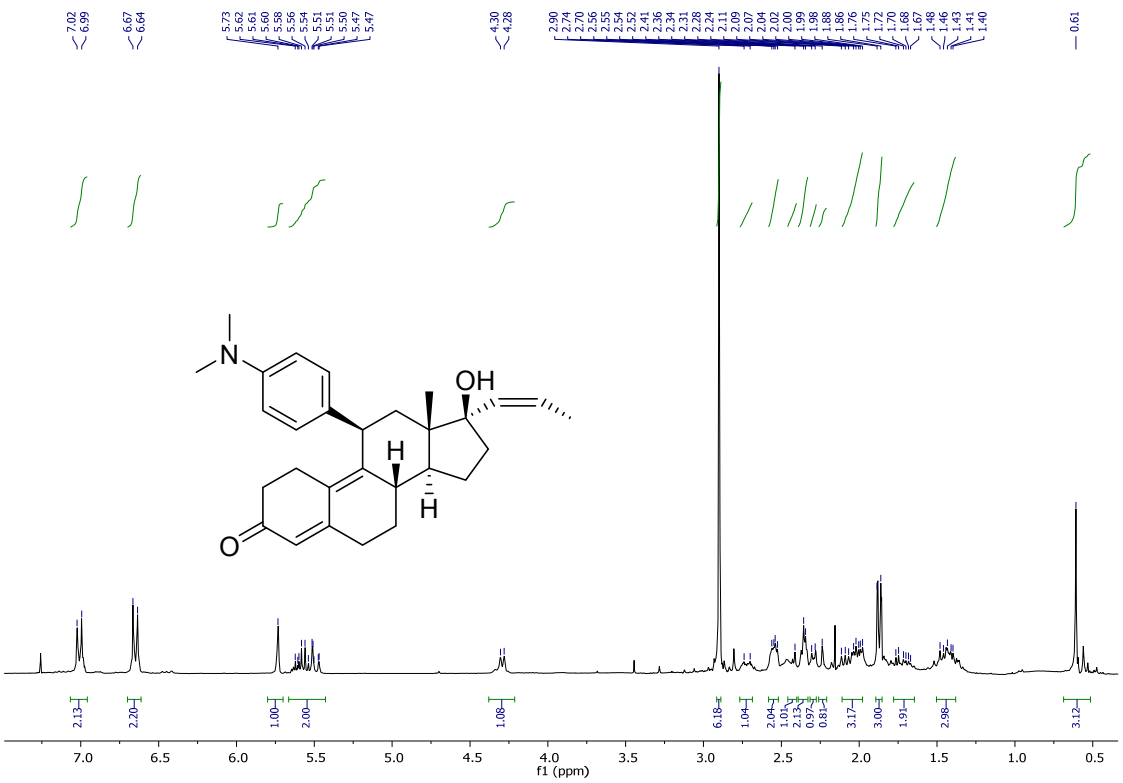

Figure S37. ^{1}H NMR of Aglepristone.

^{1}H NMR ($CDCl_3$, 300 MHz) δ 7.01 (d, *J* = *8.8 Hz*, 2H, H_{Ar}), 6.65 (d, J = 9.0 Hz, 2H, H_{Ar}), 5.73 (s, 1H, CH-C=O), 5.66 – 5.43 (m, 2H, CH=CH), 4.29 (m, 1H, CH-C_{Ar}), 2.90 (s, 6H, NCH_3), 2.72 (m, 1H, CH_2), 2.58 – 2.52 (m, 2H, CH_2), 2.41 (s, 1H, CH_2), 2.35 (m, 2H, CH_2), 2.32 – 2.28 (m, 1H, CH_2), 2.24 (m, 1H, OH), 2.01 (d, *J* = 6.0 Hz, 3H, CH_2), 1.94 – 1.83 (m, 4H, CH_2), 1.71 (m, 2H, CH_2), 1.54 – 1.33 (m, 2H), 0.61 (s, 3H).

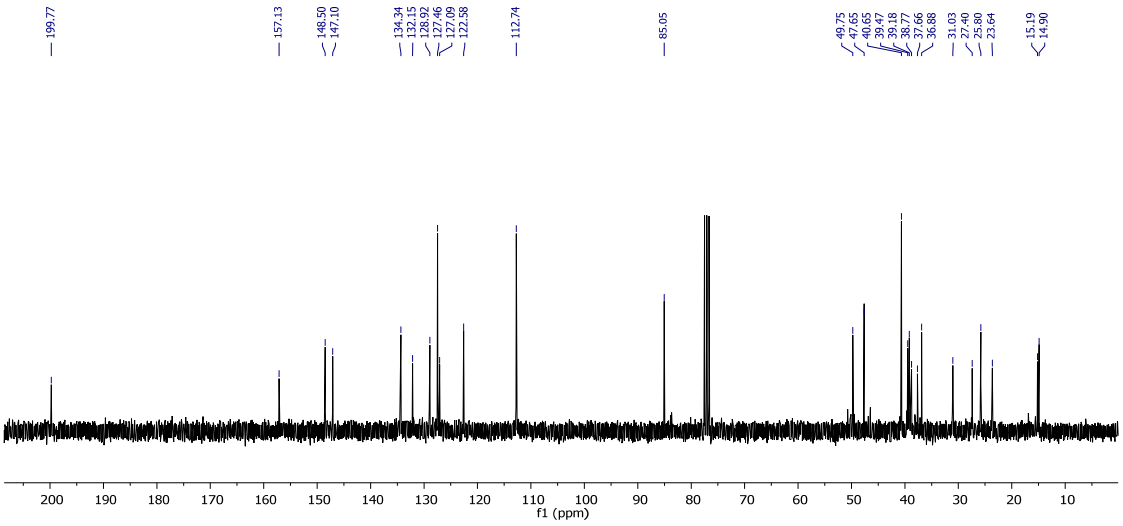

Figure S38. ^{13}C NMR of Aglepristone.

^{13}C NMR ($CDCl_3$, 75 MHz) δ 199.77 (C=O), 157.13 (**C**=C-C=O), 148.50 (C-N), 147.10 (**C**-CH-C_{Ar}), 134.34 (**C**H=CH-CH_3), 132.15, 127.46, 127.09 (CH=**C**H-

CH_3), 122.58, 112.74, 85.05 (C-OH), 49.75, 47.65, 40.65, 39.47, 39.18, 38.77, 37.66, 36.88, 31.03, 27.40, 25.80, 23.64, 15.19, 14.90 (CH_3).

c) Pd/C reduced mifepristone characterization:

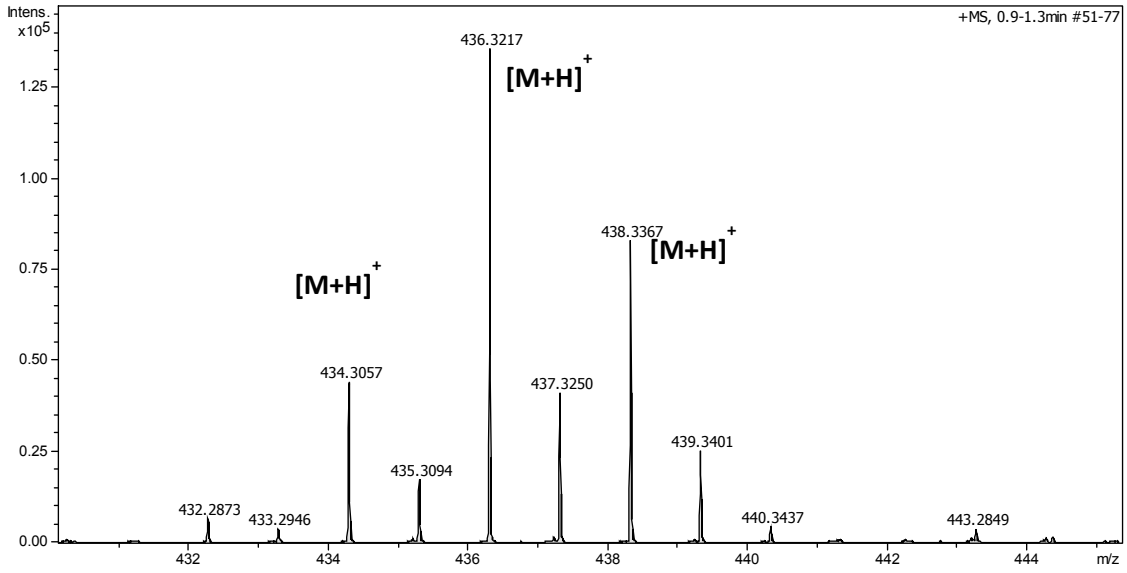

Figure S39. Mass spectra of Pd/C Reduced Mifepristone.

Meas. m/z	m/z	err [ppm]	mSigma	Ion Formula
434.3057	434.3054	-0.3	46.3	C29H40NO2
436.3217	436.3210	-1.5	293.4	C29H42NO2
438.3367	438.3367	-0.1	10.3	C29H44NO2

HRMS (ESI-TOF): **(a)** m/z calcd for $C_{29}H_{40}NO_2$ (M^+): 434.3054; found: 434.3057. **(b)** m/z calcd for $C_{29}H_{42}NO_2$ (M^+): 436.3210; found: 436.3217. **(c)** m/z calcd for $C_{29}H_{44}NO_2$ (M^+): 438.3367; found: 438.3367.

The results show the reduction to several species being the major product the reduction with six more hydrogen atoms (probably the triple bond to simple and one double bond) and in less quantity the reductions adding four and eight hydrogen atoms.

8-Bromo-7-(2-butyn-1-yl)-3-methylxanthine (Br-R) derivatives:

a) Comparison starting material- polymer reduction:

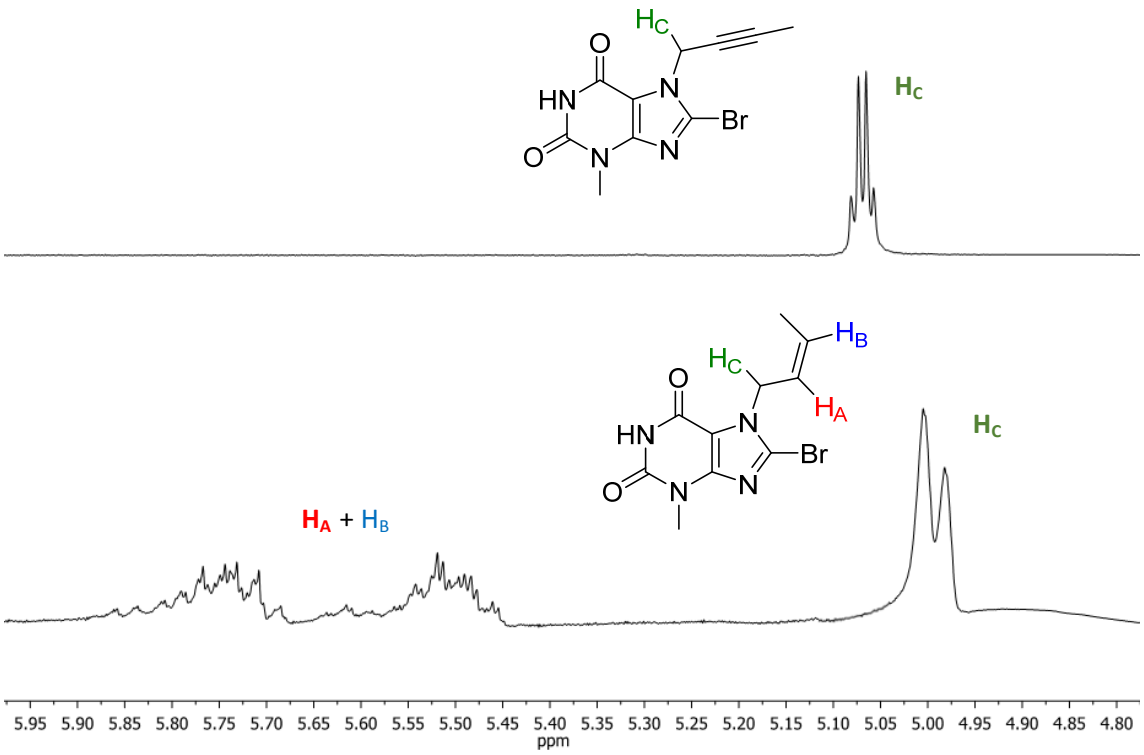

Figure S40. ^{1}H NMR comparison between Br-R and its cis reduced specie.

b) Polymer reduced Br-R characterization:

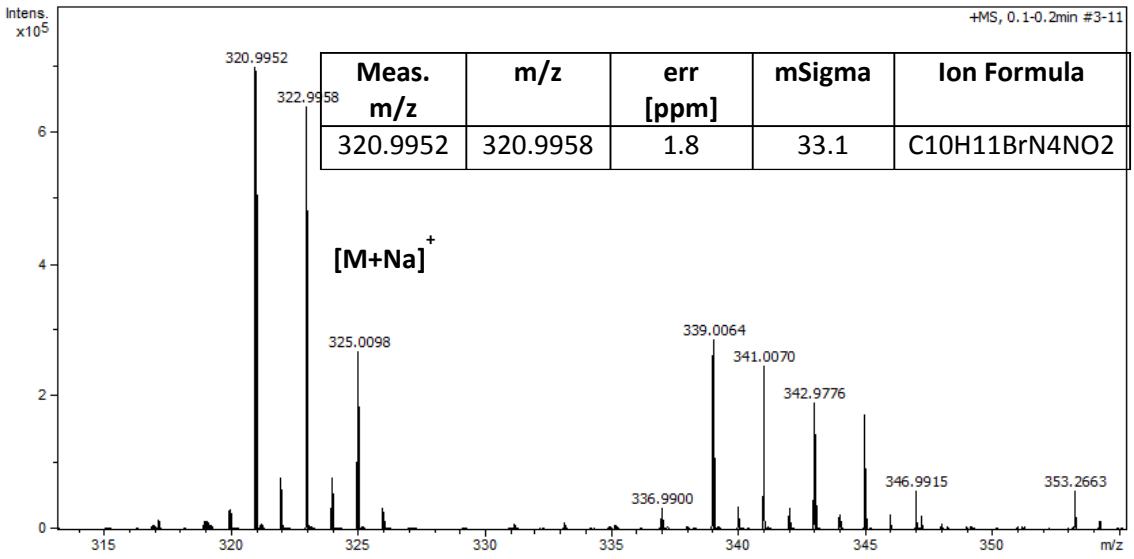

Meas. m/z	m/z	err [ppm]	mSigma	Ion Formula
320.9952	320.9958	1.8	33.1	C10H11BrN4NO2

Figure S41. Mass spectra of cis Reduced Br-R.

HRMS (ESI-TOF) m/z calcd for $C_{10}H_{11}BrN_4NaO_2$ (M^+): 320.9958; found: 320.9952.

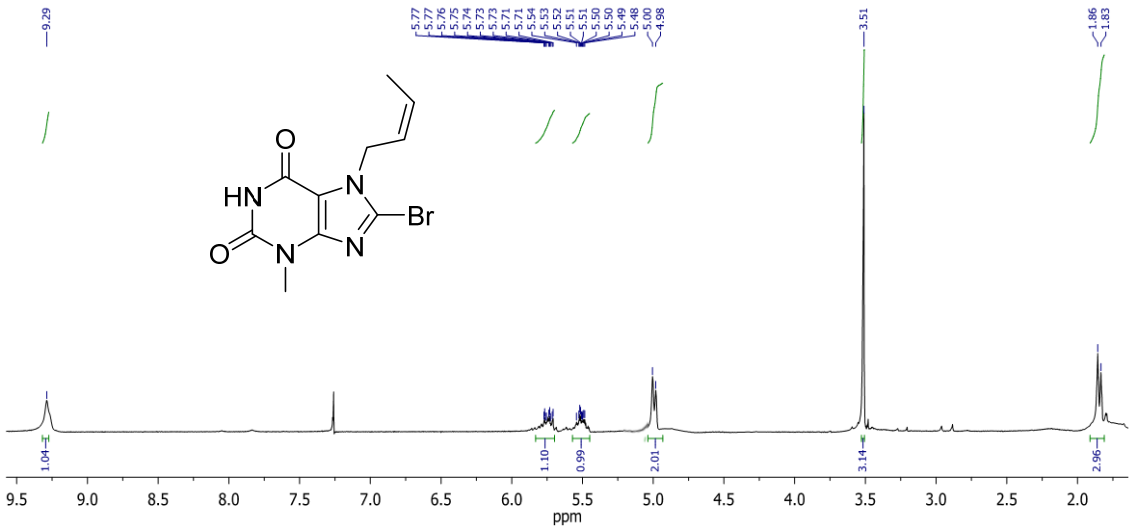

Figure S42. ^{1}H NMR of cis reduced Br-R.

^{1}H NMR ($CDCl_3$, 300 MHz) δ 9.29 (s, 1H, NH), 5.83 – 5.70 (m, 1H, CH), 5.51 (ddd, *J* = 6.9, 5.9, 3.6 Hz, 1H, CH), 4.99 (d, *J* = 6.9 Hz, 2H, CH_2), 3.51 (s, 3H, NCH_3), 1.85 (d, *J* = 7.0 Hz, 3H, CH_3).

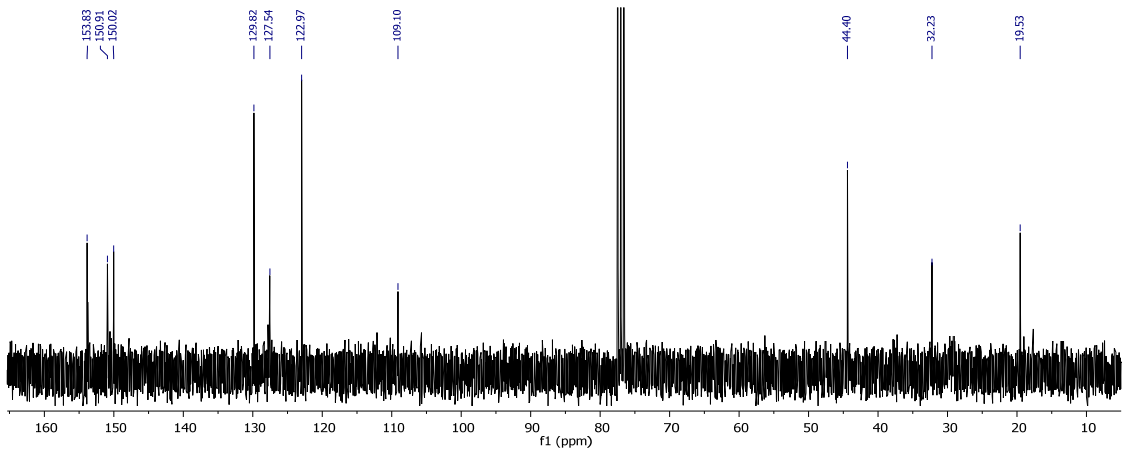

Figure S43. ^{13}C NMR of cis reduced Br-R.

^{13}C NMR (75 MHz, $CDCl_3$) δ 153.83 (C=O), 150.91 (C=O or N-C-N), 150.02 (C=O or N-C-N), 129.82 (CH), 127.54 (C-Br), 122.97 (CH), 109.10 (C_q-N), 44.40 (N-CH_3), 32.23 (CH_2), 19.53 (CH_3).

c) Pd/C reduced Br-R characterization:

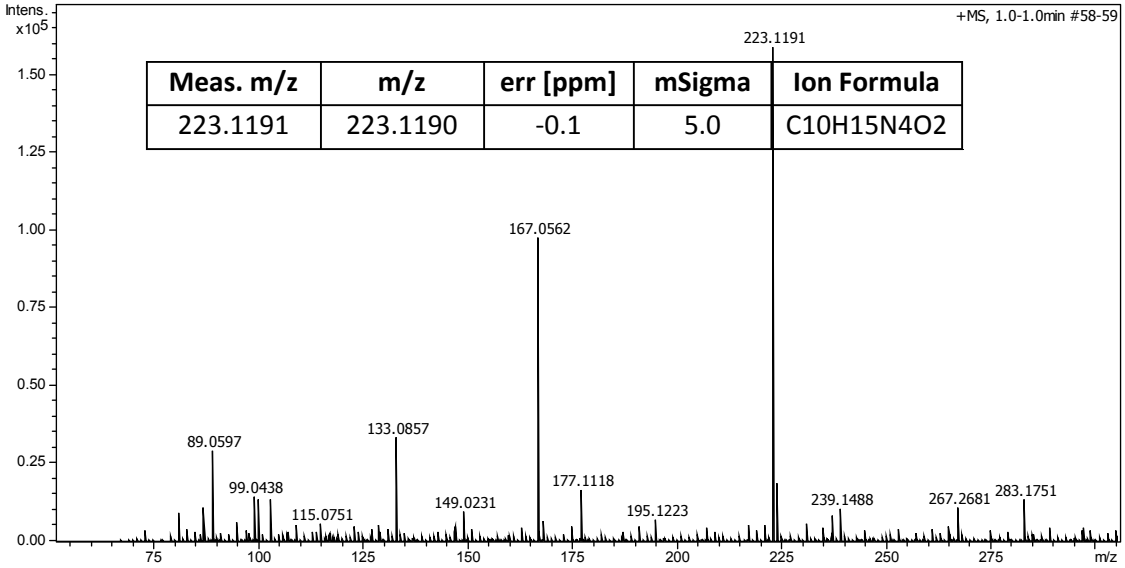

Meas. m/z	m/z	err [ppm]	mSigma	Ion Formula
223.1191	223.1190	-0.1	5.0	C10H15N4O2

Figure S44. Mass spectra of cis Reduced Br-R.

HRMS (ESI-TOF) m/z calcd for $C_{10}H_{11}BrN_4NaO_2$ (M^+): 223.1190; found: 223.1191.

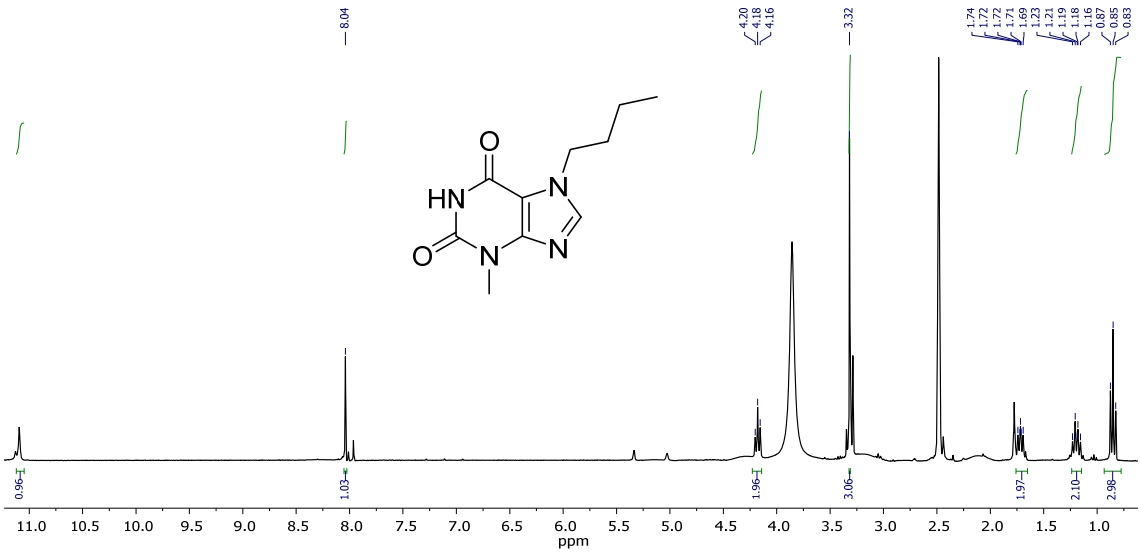

Figure S45. ^{1}H NMR of Pd/C reduced Br-R.

^{1}H NMR (DMSO-d_6, 300 MHz) δ 11.09 (s, 1H, NH), 8.04 (s, 1H, N=CH), 4.18 (t, *J* = 7.0 Hz, 2H, N-CH_2), 3.32 (s, 3H, N-CH_3), 1.75-1.69 (m, 2H, CH_2), 1.23-1.16 (m, 2H, CH_2), 0.85 (t, *J* = 7.3 Hz, 3H, CH_3).

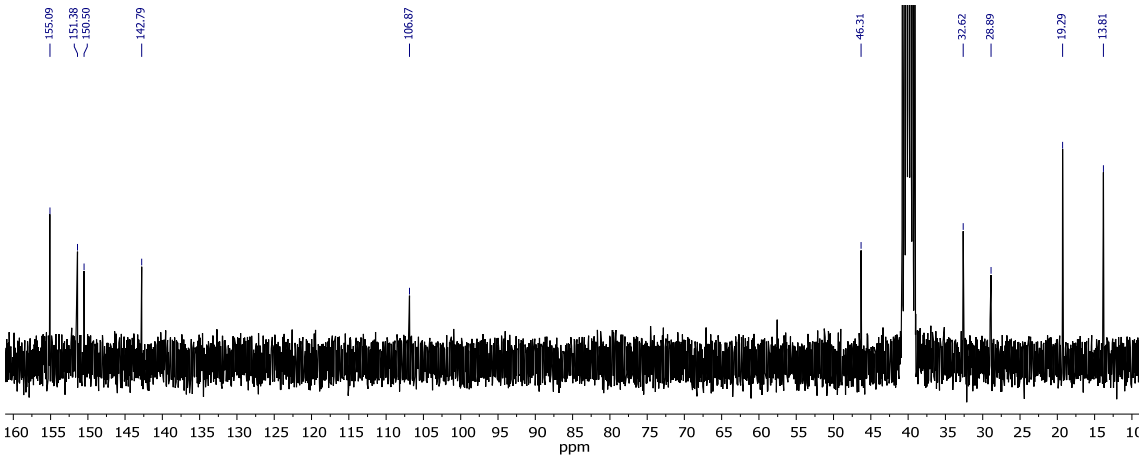

Figure S46. ^{13}C NMR of Pd/C reduced reduced Br-R.

^{13}C NMR (DMSO-d_6, 300 MHz) δ 155.09 (C=O), 151.38 (Cq), 150.50 (Cq), 142.79 (N=CH), 106.87 (N=Cq), 46.31 (N-CH_2), 32.62 (CH_3), 28.89 (CH_2), 19.29 (CH_2), 13.81 (CH_3).

Tazarotene derivatives:

a) Comparison starting material - polymer reduction:

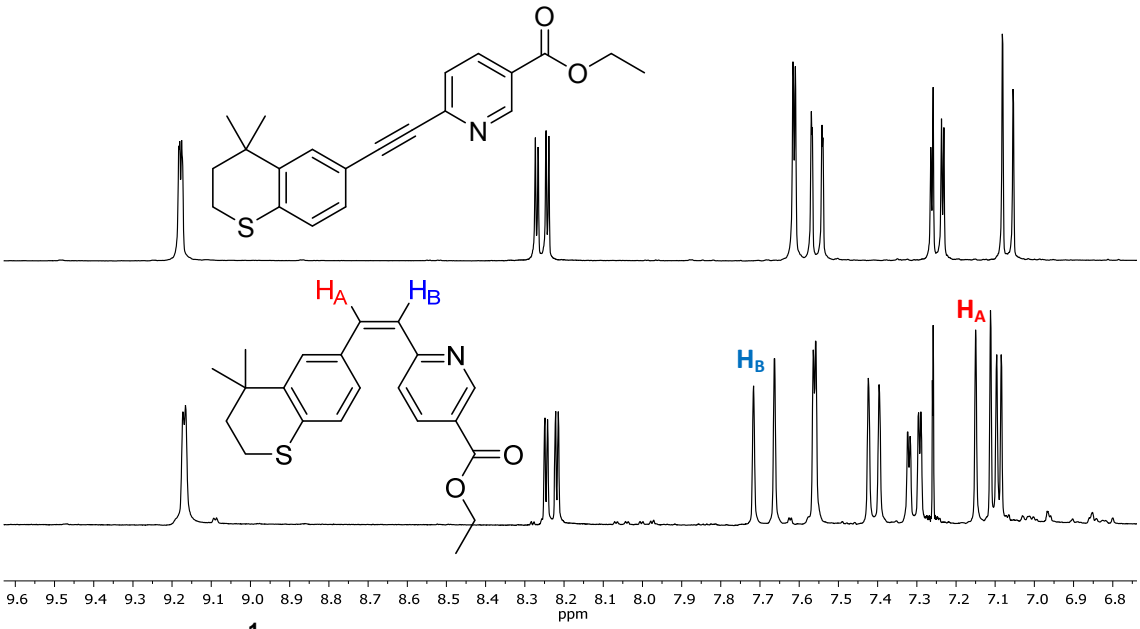

Figure S47. ^{1}HNMR comparison between tazarotene and Z-dihydro Tazarotene, its cis reduced specie.

b) Polymer reduced tazarotene characterization:

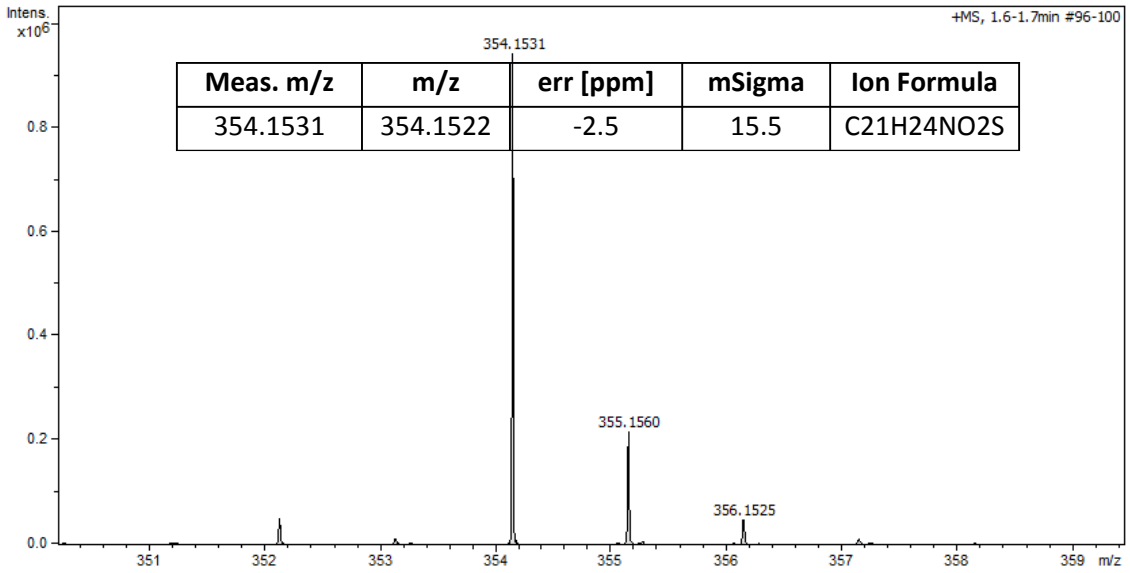

Meas. m/z	m/z	err [ppm]	mSigma	Ion Formula
354.1531	354.1522	-2.5	15.5	C21H24NO2S

Figure S48. Mass spectra of Z-dihydro Tazarotene.

HRMS (ESI-TOF) m/z calcd for $C_{21}H_{24}NO_2S$ (M^+): 354.1522; found: 354.1531.

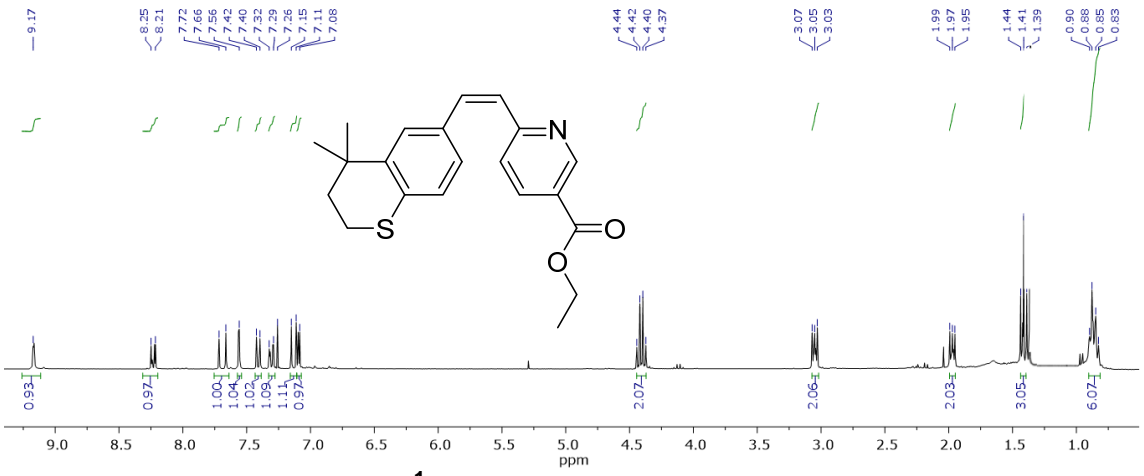

Figure S49. ^{1}H NMR of *Z*-dihydro Tazarotene.

^{1}H NMR (300 MHz, $CDCl_3$) δ 9.17 (s, 1H, N-CH_{Ar}), 8.23 (d, *J* = 10.4 Hz, 1H, H_{Ar}), 7.69 (d, *J* = 16.0 Hz, 1H, CH=CH), 7.56 (s, 1H, H_{Ar}), 7.41 (d, *J* = 8.2 Hz, 1H, H_{Ar}), 7.31 (d, *J* = 10.1 Hz, 1H, H_{Ar}), 7.11 (d, *J* = 10.4 Hz, 1H, CH=CH), 7.08 (m, 1H, H_{Ar}), 4.41 (q, *J* = 7.1 Hz, 2H, O-CH_2), 3.07 – 3.02 (m, 2H, SCH_2), 1.99 – 1.95 (m, 2H, CH_2), 1.42 (m, 3H, CH_3), 0.90 – 0.81 (m, 6H, CCH_3).

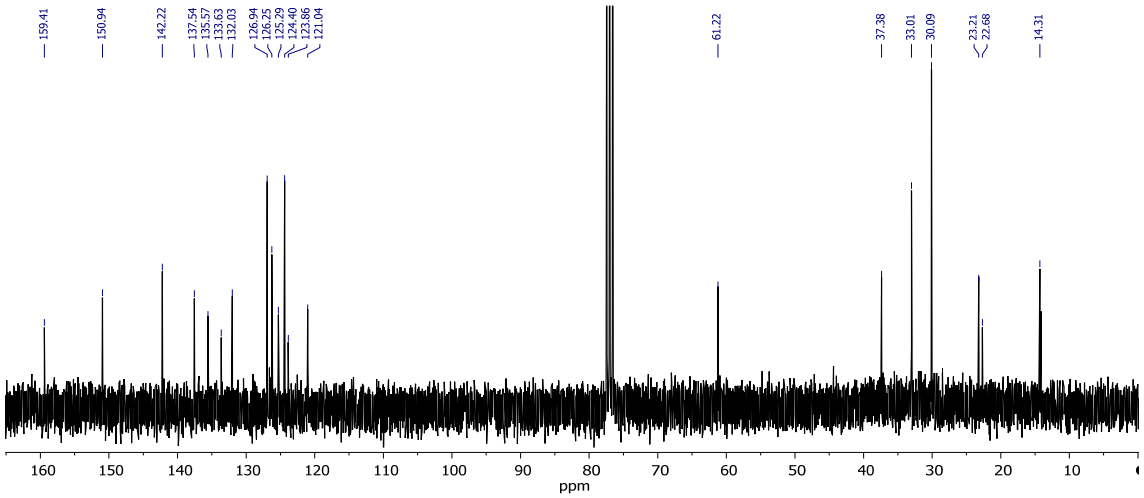

Figure S50. ^{13}C NMR of *Z*-dihydro Tazarotene.

^{13}C NMR (75 MHz, $CDCl_3$) δ 159.41 (C=O), 150.94 (C_{Ar}-N), 142.22 (C_{Ar}), 137.54 ($C_{Ar}H$), 135.57 ($C_{Ar}H$), 132.03 ($C_{Ar}H$), 126.94 ($C_{Ar}H$), 126.25 ($C_{Ar}H$), 125.29 ($C_{Ar}H$), 124.40 ($C_{Ar}H$), 123.86 (C_{Ar}), 121.04 ($C_{Ar}H$), 61.22 (CH_2), 37.38 (CH_2), 33.01 (C_q), 30.09 (CH_3), 23.21 (CH_2), 22.68 (CH_2), 14.31 (CH_3).

c) Pd/C reduced tazarotene characterization:

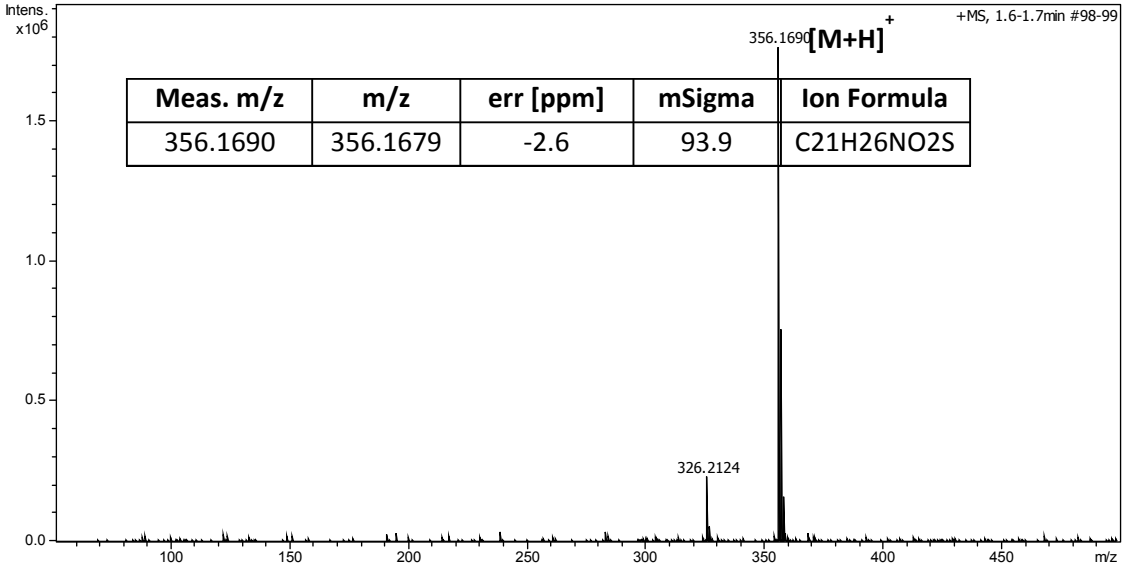

Meas. m/z	m/z	err [ppm]	mSigma	Ion Formula
356.1690	356.1679	-2.6	93.9	C21H26NO2S

Figure S51. Mass spectra of Pd/C reduced Tazarotene.

HRMS (ESI-TOF) m/z calcd for $C_{21}H_{26}NO_2S$ (M^+): 356.1679; found: 356.1690.

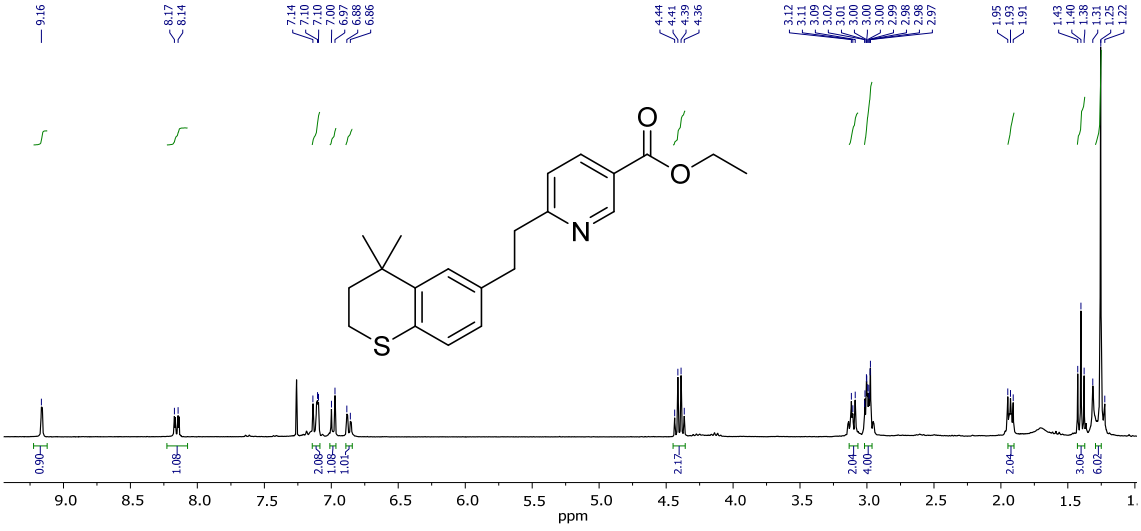

Figure S52. ^{1}H NMR of Pd/C reduced Tazarotene.

^{1}H NMR (300 MHz, $CDCl_3$) δ 9.16 (s, 1H, N=CH_{Ar}), 8.16 (d, *J* = 8.1, 1H, CH_{Ar}), 7.14 – 7.08 (m, 2H), 6.99 (d, *J* = 8.0 Hz, 1H), 6.87 (d, *J* = 8.0 Hz, 1H, CH_{Ar}), 4.40 (q, *J* = 7.1 Hz, 2H, OCH_2), 3.13 – 3.07 (m, 2H, CH_2), 3.02 – 2.96 (m, 4H, CH_2), 1.95 – 1.90 (m, 2H, CH_2), 1.40 (t, *J* = 7.1 Hz, 3H, CH_3), 1.31-1.22 (m, 6H, CH_3).

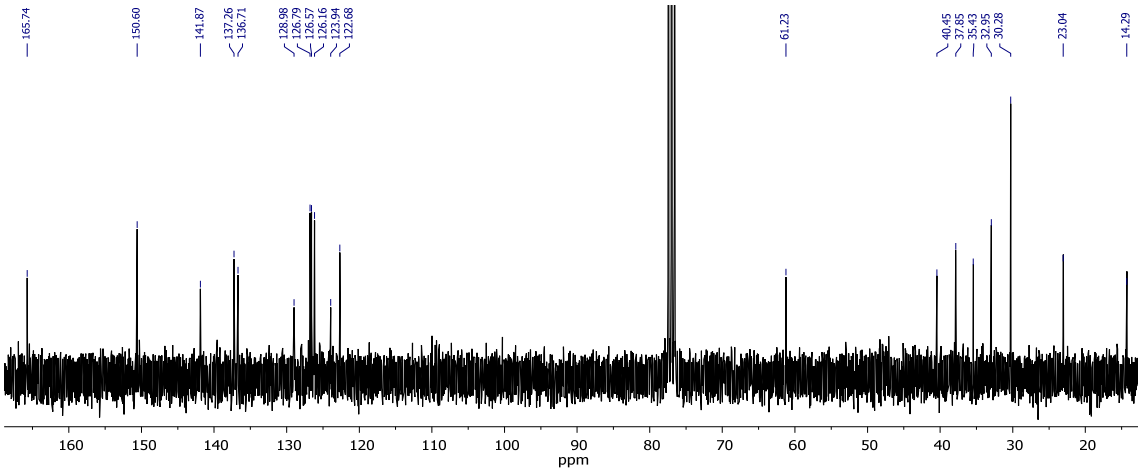

Figure S53. ^{13}C NMR of Pd/C reduced Tazarotene.

^{13}C NMR (75 MHz, $CDCl_3$) δ 165.74 (C=O), 150.60 ($C_{Ar}H$), 141.87 (C_{Ar}), 137.26 ($C_{Ar}H$), 136.71 (C_{Ar}), 128.98 (C_{Ar}), 126.79 ($C_{Ar}H$), 126.57 ($C_{Ar}H$), 126.16 ($C_{Ar}H$) , 123.94 (C_{Ar}), 122.68 ($C_{Ar}H$), 61.23 (CH_2), 40.45 (CH_2), 37.85 (CH_2), 35.43 (Cq), 32.95 (CH_2), 30.28 (CH_3), 23.04 (CH_2), 14.29 (CH_3).

Pentacosa-10,12-diynoic acid (2t-Lipo):

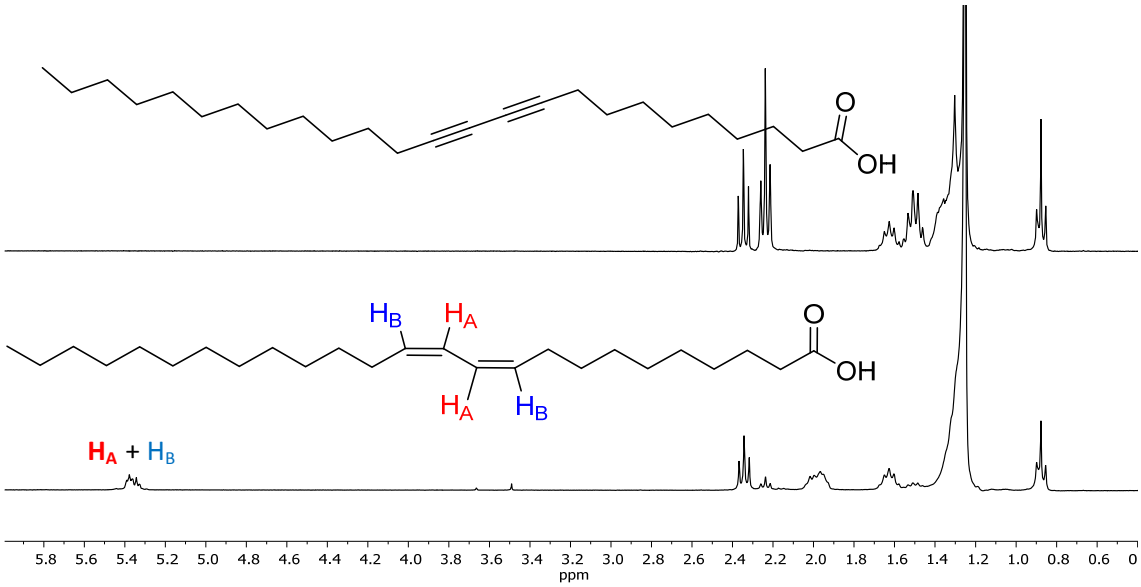

Figure S54. ^{1}HNMR comparison between 2t-Lipo and the analysis performed for the product of reduction with H_2 and Pd@PB80_20A4.

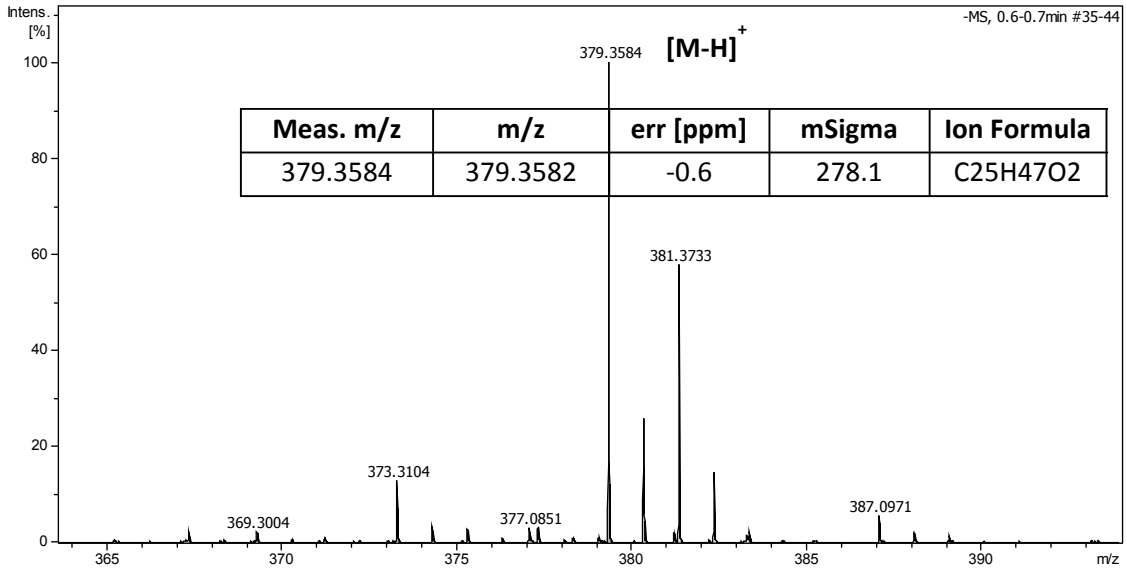

Figure S55. Mass spectra of cis reduced 2t-Lipo.

HRMS (ESI-TOF) m/z calcd for $C_{25}H_{47}O_2$ (M^+): 379.3582; found: 379.3584.

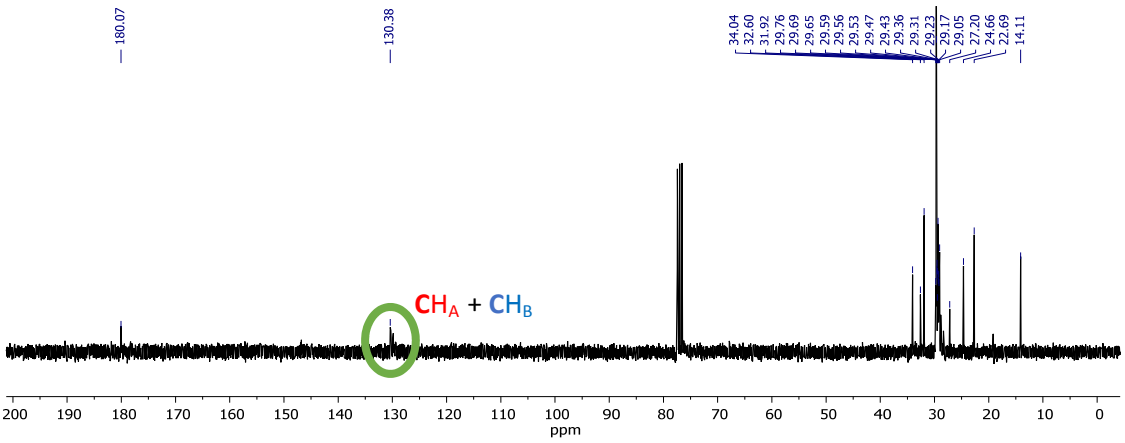

Figure S56. ^{13}C NMR spectrum performed for the product of reduction of 2t-Lipo with H_2 and Pd@PB80_20A4.

a) Pd/C reduced 2t-Lipo characterization:

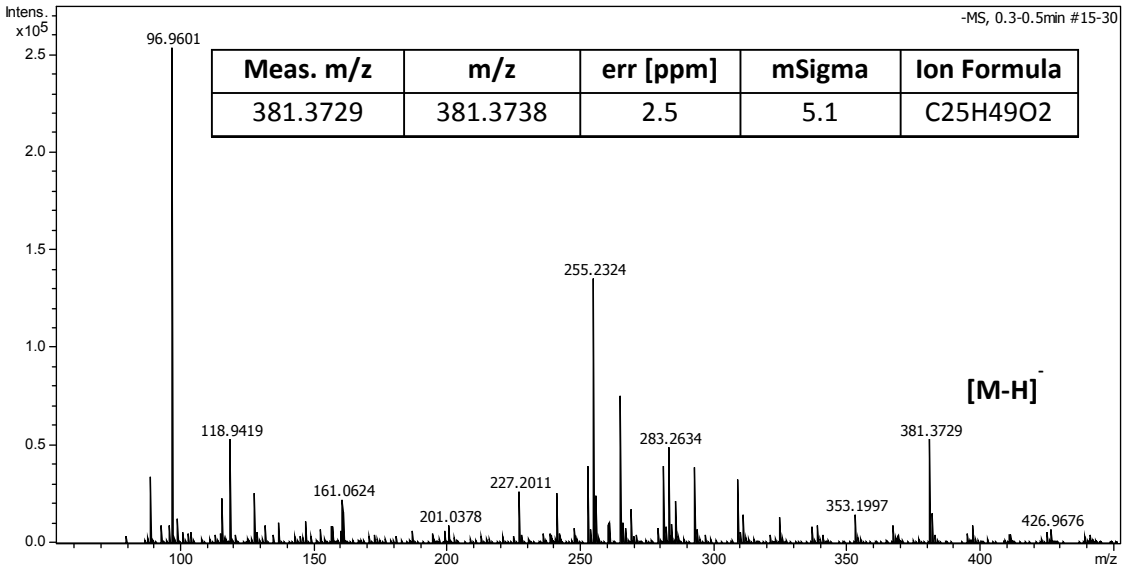

Meas. m/z	m/z	err [ppm]	mSigma	Ion Formula
381.3729	381.3738	2.5	5.1	C25H49O2

Figure S57. Mass spectra of Pd/C reduced 2t-Lipo.

HRMS (ESI-TOF) m/z calcd for $C_{25}H_{49}O_2$ (M^+): 381.3738; found: 381.3729.

Comparison with Lindlar catalyst:

Two different series of experiments were performed:

- In the first series of experiments, the conditions were similar to the used for the semihydrogenation performed with Pd@PB80_20A4:
  - 30 mg of the reagent to reduce.
  - 3 mL of solvent.
  - 30 mg of Lindlar catalyst.
  - 15 hours at 5 atm of H_2.

MeOH	Efavirenz	Mifepristone	Tazarotene	Br-R
Z-reduced	80	80	28	24
Alkyne to alkane	10	15	20	51
Other products*	10	5	52	25

Figure S58. Products of hydrogenation reactions of efavirenz, mifepristone, tazarotene and the xanthine derivative (Br-R) in MeOH with Lindlar catalyst in MeOH.

  - For Mifepristone, other products were obtained, including the product from a third reduction, that it was likely to be from the 1,4-diene as it happened when using Pd/C 10%.
  - Efavirenz afforded several by products, including the loss of the chlorine atom; additionally, another major product was the Z-reduction and the opening of the cyclopropyl group.
  - In the case of Tazarotene a major by-product was identified as the 2+2 cycloaddition of the semihydrogenation product, detected by its signal in the QTOF mass spectrum (6545 Q-TOF (Agilent)). The percentage of every product was calculated from the NMR spectra.

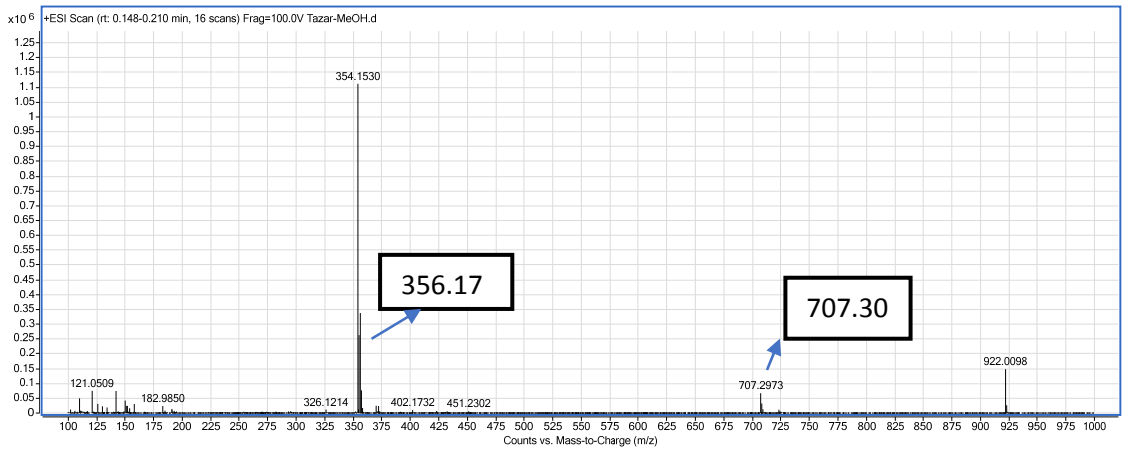

Figure S59. Mass spectra of tazarotene reduced with Lindlar catalyst in MeOH solution. Inset: m/z = 356.17 (*Z*-Hydrogenation) and m/z = 707.30 (2+2 cycloaddition).

- For Br-R the major by-product was the reduction to *Z*-semihydrogenation and the loss of the bromine atom.

- In the second series of experiments, we used THF as solvent (3 mL) adding quinoline (12 µL) to improve the formation of the cis product.

THF + Quinoline	Efavirenz	Mifepristone	Tazarotene	Br-R
***Z*-reduced**	90	100	85	95
Alkyne to alkane	0	0	0	5
Other products	10	0	15	0

Figure S60. Products of hydrogenation reactions of efavirenz, mifepristone, tazarotene and the xanthine derivative (Br-R) in MeOH with Lindlar catalyst in THF+Quinoline.

The results were closely related to the ones obtained with the polymer catalyst Pd@PB80_20A4.

Due to the results observed, we concluded that there was a relation between the conditions–catalyst that led to the different products:

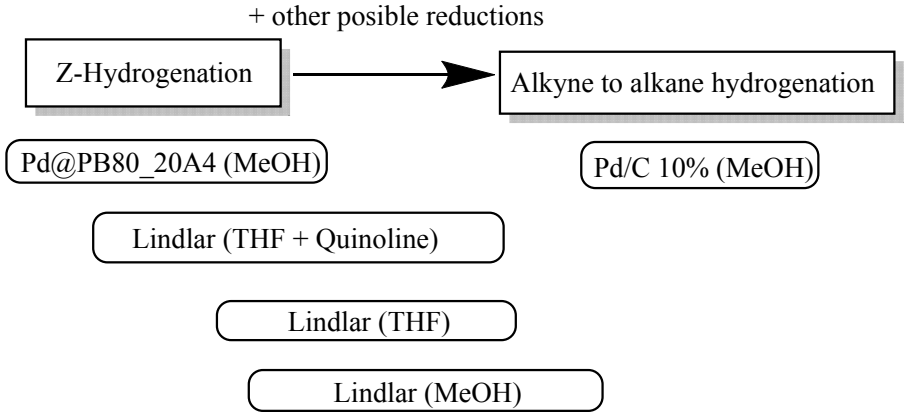

*Other possible competitive processes included, for example, dehalogenation, reduction of 1-4 dienes, the *E*-hydrogenation products or the 2+2 cycloaddition.

Figure S61. Schematic representation of the products obtained depending on the hydrogenation

In conclusion:

- Higher selectivity for the *Z*-Hydrogenated product was found when using Pd@PB80_20A4 in MeOH.
- The results were similar when using the Lindlar catalyst in THF+Quinoline. However, this was not a green process.
- Pd@PB80_20A4 presented easier recyclability, not possible for the Lindlar catalyst.

4. DFT CALCULATIONS:

Table S1. Cartesian coordinates (Å) of model of mifepristone interacting with Pd_{10} layer, A.

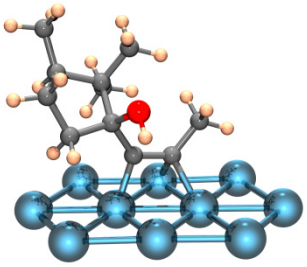

C	-0.424164	-1.383944	-2.260887
C	0.792502	-0.712884	-1.506270
C	1.966319	-0.606925	-2.490984
C	-1.399806	-0.440744	-2.964136
C	-1.068358	-2.327901	-1.242835
C	0.150318	-2.927486	-0.555897
C	1.066359	-1.718326	-0.259950
H	-1.714366	-3.084630	-1.716883
H	0.668975	-3.625751	-1.247434
H	0.019758	-2.029839	-3.040504
O	0.577286	-1.065927	0.917207
H	0.719835	-1.675768	1.659620
C	2.528744	-2.087777	0.046424
C	3.552002	-1.285807	0.559892
C	0.429949	0.699903	-1.006309
H	-0.480306	0.706111	-0.392932
H	1.232178	1.130071	-0.395831
H	0.271064	1.368814	-1.865989
C	3.479944	0.214260	0.743813
H	2.655032	0.458831	1.432284
H	4.413092	0.624997	1.176318
H	3.300854	0.725659	-0.213501
H	-1.681909	-1.764460	-0.518854
H	-0.057002	-3.492412	0.369897
H	-2.121811	-1.022864	-3.560601
H	-0.884706	0.247203	-3.655300
H	-1.977152	0.170465	-2.252183
H	1.641311	-0.056684	-3.388748
H	2.323040	-1.600810	-2.816879
H	2.829793	-0.071665	-2.070356
Pd	1.862801	-5.513800	-1.617300
Pd	1.227000	-5.726800	1.101200
Pd	3.158796	-3.884898	0.255401
Pd	4.465902	-2.270601	2.124099
Pd	2.490801	-4.066601	2.968500
Pd	3.802500	-2.447400	4.838600
Pd	5.775800	-0.652700	3.996800
Pd	3.794600	-3.671900	-2.463100
Pd	5.103301	-2.056601	-0.590900
Pd	6.362699	-0.395799	1.271100

Table S2. Cartesian coordinates (Å) of model of hydrogenated mifepristone interacting with Pd_{10} layer (Hydrogen atoms oriented towards the opposite side of OH group), B.

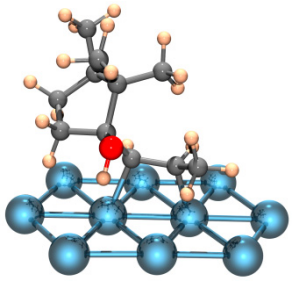

C	0.966020	-0.344154	-2.123347
C	0.326338	-0.419978	-0.695356
C	0.774420	0.789320	0.140181
C	0.377477	0.696296	-3.077486
C	0.926255	-1.790032	-2.684179
C	0.498110	-2.678332	-1.512911
C	0.773590	-1.895570	-0.203221
H	1.924878	-2.090769	-3.063743
H	1.010706	-3.665313	-1.510498
H	2.022975	-0.064124	-1.972435
O	-0.073809	-2.341123	0.837295
H	0.229387	-3.235708	1.083534
C	2.268822	-1.943315	0.231123
C	2.741142	-1.286380	1.504682
C	-1.216688	-0.374068	-0.751088
H	-1.647354	-1.068382	-1.486807
H	-1.641540	-0.623615	0.230802
H	-1.553093	0.638394	-1.022095
C	1.819612	-1.105949	2.699635
H	1.480649	-2.068047	3.136786
H	2.326456	-0.522610	3.482963
H	0.892913	-0.587685	2.412971
H	0.233413	-1.883753	-3.536056
H	-0.579942	-2.886158	-1.531044
H	0.950201	0.713351	-4.019250
H	0.418256	1.713798	-2.654168
H	-0.670869	0.475365	-3.335698
H	0.495038	1.712660	-0.393053
H	1.860241	0.828948	0.303318
H	0.273524	0.827361	1.117227
Pd	1.862800	-5.513800	-1.617300
Pd	1.227000	-5.726800	1.101200
Pd	3.158800	-3.884900	0.255400
Pd	4.465900	-2.270600	2.124100
Pd	2.490800	-4.066600	2.968500
Pd	3.802500	-2.447400	4.838600
Pd	5.775800	-0.652700	3.996800
Pd	3.794600	-3.671900	-2.463100
Pd	5.103300	-2.056600	-0.590900
Pd	6.362700	-0.395800	1.271100
H	2.884450	-1.555004	-0.607405
H	3.274190	-0.349276	1.276823

Table S3. Cartesian coordinates (Å) of model of hydrogenated mifepristone interacting with Pd_{10} layer (Hydrogen atoms oriented towards the side of OH group), C.

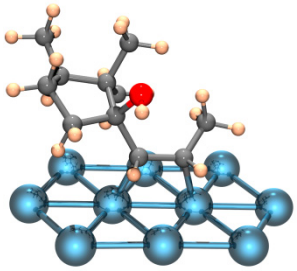

C	0.674956	-1.470154	-2.899607
C	1.405572	-0.712224	-1.725449
C	2.905582	-0.630063	-2.040188
C	0.353352	-0.665815	-4.159718
C	-0.545854	-2.124466	-2.245775
C	0.050120	-2.677055	-0.962477
C	0.977603	-1.563947	-0.415596
H	-1.006911	-2.899404	-2.879954
H	0.652125	-3.582641	-1.190859
H	1.352949	-2.299059	-3.191930
O	0.165033	-0.668273	0.375498
H	-0.295271	-1.200224	1.039016
C	1.963723	-2.175963	0.644237
C	2.712200	-1.301081	1.623285
C	0.898309	0.745777	-1.625908
H	-0.194847	0.809205	-1.545270
H	1.319148	1.252993	-0.748927
H	1.212477	1.309670	-2.517636
C	2.996267	0.168842	1.374070
H	2.041872	0.684499	1.174625
H	3.454250	0.616430	2.267419
H	3.674800	0.355055	0.531675
H	-1.320855	-1.368424	-2.028340
H	-0.687966	-2.977248	-0.199617
H	-0.063980	-1.331478	-4.933244
H	1.244424	-0.181824	-4.592508
H	-0.393984	0.119749	-3.968155
H	3.057858	-0.246738	-3.062056
H	3.386800	-1.648824	-2.007212
H	3.446419	0.041950	-1.361696
Pd	1.862800	-5.513800	-1.617300
Pd	1.227000	-5.726800	1.101200
Pd	3.158802	-3.884902	0.255400
Pd	4.465899	-2.270599	2.124100
Pd	2.490800	-4.066600	2.968500
Pd	3.802500	-2.447400	4.838600
Pd	5.775800	-0.652700	3.996800
Pd	3.794600	-3.671900	-2.463100
Pd	5.103300	-2.056600	-0.590900
Pd	6.362700	-0.395800	1.271100
H	1.288162	-2.813103	1.251766
H	2.247100	-1.414822	2.620140

Reference

[1] Ganesan, M.; Freemantle, R. G.; Obare, S. O. Approaches to Synthesis and Characterization of Spherical and Anisotropic Palladium Nanomaterials, *Chem. Mater.* **2007**, *19*, 3464–3471.